

Recent advances in neutrinoless double beta decay with energy density functional methods

Tomás R. Rodríguez



TECHNISCHE
UNIVERSITÄT
DARMSTADT

**Congratulations to Alfredo, Andrés, Etienne and all the people
from Strasbourg-Madrid (SM) collaboration!!**

Recent advances in neutrinoless double beta decay with energy density functional methods

Tomás R. Rodríguez



TECHNISCHE
UNIVERSITÄT
DARMSTADT

Outline



TECHNISCHE
UNIVERSITÄT
DARMSTADT

- 1. Introduction: $0\nu\beta\beta$ decay**
- 2. Method: GCM+PNAMP**
- 3. Results**
- 4. Summary and Conclusions**

Outline



TECHNISCHE
UNIVERSITÄT
DARMSTADT

1. Introduction: $0\nu\beta\beta$ decay

**Perrot's and
Menéndez's talk!**

2. Method: GCM+PNAMP

3. Results

4. Summary and Conclusions

Outline



TECHNISCHE
UNIVERSITÄT
DARMSTADT

1. Introduction: $0\nu\beta\beta$ decay

**Perrot's and
Menéndez's talk!**

2. Method: GCM+PNAMP

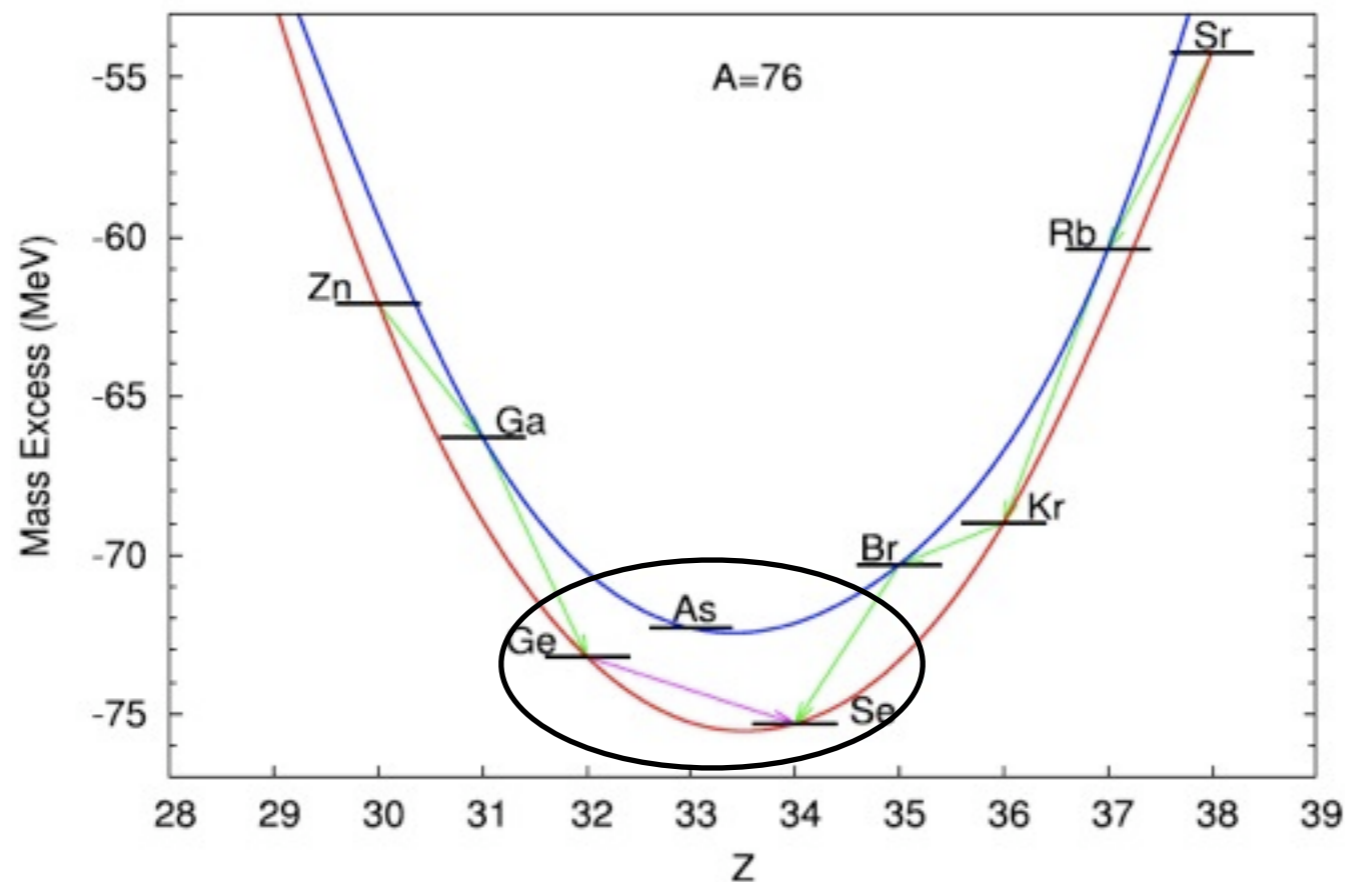
Robledo's talk!

3. Results

4. Summary and Conclusions

Double beta decay

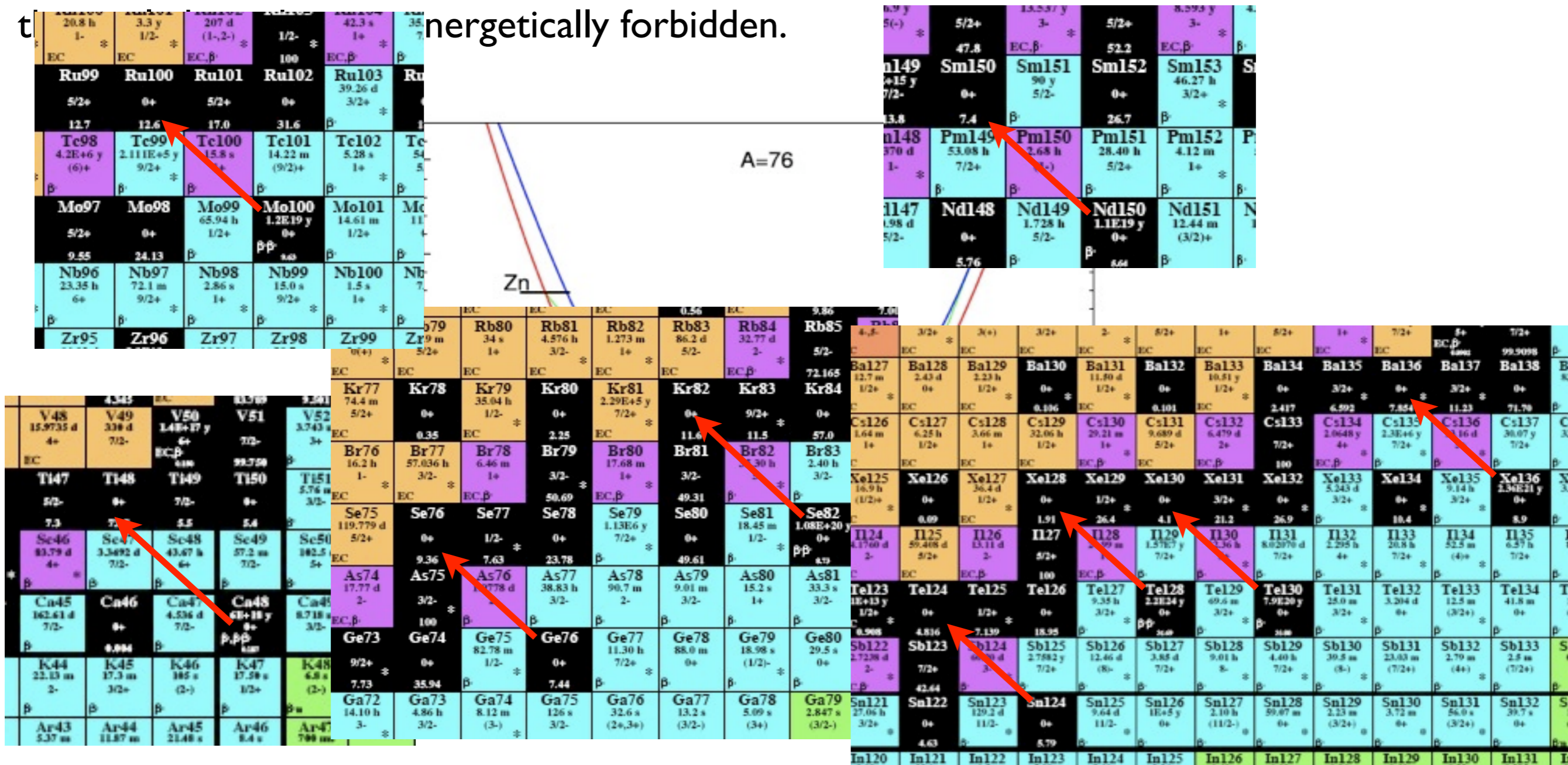
Process mediated by the weak interaction which occurs in those even-even nuclei where the single beta decay is energetically forbidden.



taken from J. Menéndez

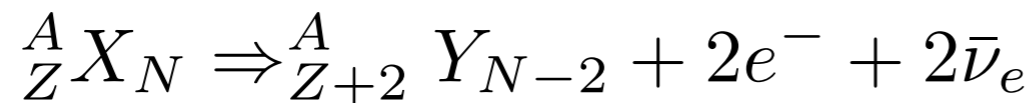
Double beta decay

Process mediated by the weak interaction which occurs in those even-even nuclei where $\beta\beta$ is energetically forbidden.



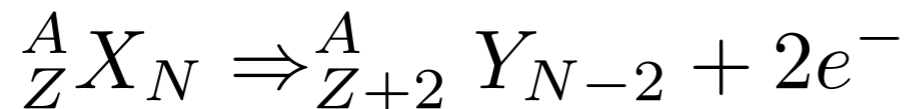
Double beta decay

Two neutrino double beta decay $2\nu\beta\beta$



- Conserves the leptonic number
- Compatible with massive or massless Dirac/Majorana neutrinos
- Experimentally observed ($T_{1/2} \sim 10^{19-21}$ y)
- Within the Standard Model

Neutrinoless double beta decay $0\nu\beta\beta$



- Violates the leptonic number conservation
- Neutrinos are massive Majorana particles
- Experimentally not observed (yet?) ($T_{1/2} > 10^{25}$ y)
- Beyond the Standard Model

Double beta decay

Half-life neutrinoless double beta decay (Doi et al (1985))

$$\left(T_{1/2}^{0\nu\beta\beta}(0^+ \rightarrow 0^+) \right)^{-1} = G_{01} |M^{0\nu\beta\beta}|^2 \left(\frac{\langle m_\nu \rangle}{m_e} \right)^2$$

light-neutrino exchange mechanism

- Kinematic phase space factor:

$$G_{01} = \frac{(Gg_A(0))^4 m_e^4}{64\pi^5 \ln 2} \int F_0(Z, \varepsilon_1) F_0(Z, \varepsilon_2) \times p_1 p_2 \delta(\varepsilon_1 + \varepsilon_2 - E_f - E_i) d\varepsilon_1 d\varepsilon_2 d(\hat{p}_1 \cdot \hat{p}_1)$$

- Effective neutrino mass:

$$\langle m_\nu \rangle = \sum_j U_{ej}^2 m_j$$

- Nuclear Matrix Element (NME):

$$M^{0\nu\beta\beta} = - \left(\frac{g_V(0)}{g_A(0)} \right)^2 M_F^{0\nu\beta\beta} + M_{GT}^{0\nu\beta\beta} - M_T^{0\nu\beta\beta}$$

Fermi Gamow-Teller Tensor

Nuclear Matrix Elements

$$M^{0\nu\beta\beta} = - \left(\frac{g_V(0)}{g_A(0)} \right)^2 M_F^{0\nu\beta\beta} + M_{GT}^{0\nu\beta\beta} - M_T^{0\nu\beta\beta}$$

- Each term can be written as the expectation value of a transition operator acting on the initial and final states:

$$M_\xi^{0\nu\beta\beta} = \langle 0_f^+ | \hat{O}_\xi^{0\nu\beta\beta} | 0_i^+ \rangle$$

- Nuclear structure methods for calculating these NME:
 - Quasiparticle Random Phase Approximation in different versions: QRPA, RQRPA, SRQRPA. (Tübingen group, Jyväskylä group)
 - Interacting Shell Model -ISM- (Strasbourg-Madrid collaboration, Michigan)
 - Interacting Boson Model -IBM- (Yale group)
 - Projected Hartree-Fock-Bogoliubov -PHFB- (Lucknow-UNAM group)
 - Energy Density Functional

Nuclear Matrix Elements

$$M^{0\nu\beta\beta} = - \left(\frac{g_V(0)}{g_A(0)} \right)^2 M_F^{0\nu\beta\beta} + M_{GT}^{0\nu\beta\beta} - M_T^{0\nu\beta\beta}$$

- Each term can be written as the expectation value of a transition operator acting on the initial and final states:

$$M_\xi^{0\nu\beta\beta} = \langle 0_f^+ | \hat{O}_\xi^{0\nu\beta\beta} | 0_i^+ \rangle$$

- Nuclear structure methods for calculating these NME:

Different ways to deal with:

- Finding the best initial and final ground states.
- Handling the transition operator (inclusion of most relevant terms, corrections, approximations, etc.).

Some remarks about these methods:

- Calculations with limited single particle bases.
- Interactions fitted to the specific region (ISM) or to each nucleus individually (rest).
- Difficulties to include collective degrees of freedom.
- Problems with particle number conservation.

Method: GCM+PNAMP

- **Effective nucleon-nucleon interaction:**

Gogny force (DIS-DIM) that is able to describe properly many phenomena along the whole nuclear chart.

$$V(1, 2) = \sum_{i=1}^2 e^{-(\vec{r}_1 - \vec{r}_2)^2 / \mu_i^2} (W_i + B_i P^\sigma - H_i P^\tau - M_i P^\sigma P^\tau) \\ + iW_0(\sigma_1 + \sigma_2) \vec{k} \times \delta(\vec{r}_1 - \vec{r}_2) \vec{k} + t_3(1 + x_0 P^\sigma) \delta(\vec{r}_1 - \vec{r}_2) \rho^\alpha ((\vec{r}_1 + \vec{r}_2)/2) \\ + V_{\text{Coulomb}}(\vec{r}_1, \vec{r}_2)$$

- **Method of solving the many-body problem:**

First step: Particle Number Projection (before the variation) of HFB-type wave functions.

Second step: Simultaneous **Particle Number and Angular Momentum Projection** (after the variation).

Third step: Configuration mixing within the framework of the **Generator Coordinate Method (GCM)**.

Particle number projection

Determination of initial and final states (I)

Intrinsic state: Solve the PN-VAP equations with the Gogny DIS/DIM interaction

$$|\Phi\rangle \text{ HFB states } \longrightarrow \delta(E^{N,Z} [|\bar{\Phi}(q)\rangle])_{|\bar{\Phi}\rangle=|\Phi\rangle} = 0$$

$$E^{N,Z} [|\Phi\rangle] = \frac{\langle \Phi | \hat{H} \hat{P}^N \hat{P}^Z | \Phi \rangle}{\langle \Phi | \hat{P}^N \hat{P}^Z | \Phi \rangle} + \varepsilon_{DD}^{N,Z} (|\Phi\rangle) - \lambda_q \langle \Phi | \hat{Q} | \Phi \rangle$$

Particle number and angular momentum projected state:

$$|IMK; NZ; q\rangle = \frac{2I+1}{8\pi^2} \int \mathcal{D}_{MK}^{I*}(\Omega) \hat{R}(\Omega) \hat{P}^N \hat{P}^Z |\Phi(q)\rangle d\Omega$$

General form (GCM state):

$$|IM; NZ\sigma\rangle = \sum_{Kq} f_{Kq}^{I;NZ,\sigma} |IMK; NZ; q\rangle$$

Hill-Wheeler-Griffin equation (GCM)

$$\sum_{K'q'} \left(\mathcal{H}_{KqK'q'}^{I;NZ} - E^{I;NZ;\sigma} \mathcal{N}_{KqK'q'}^{I;NZ} \right) f_{K'q'}^{I;NZ;\sigma} = 0$$

$$\mathcal{N}_{KqK'q'}^{I;NZ} \equiv \langle IMK; NZ; q | IMK'; NZ; q' \rangle$$

$$\mathcal{H}_{KqK'q'}^{I;NZ} \equiv \langle IMK; NZ; q | \hat{H} | IMK'; NZ; q' \rangle + \varepsilon_{DD}^{IKK';NZ} [|\Phi(q)\rangle, |\Phi(q')\rangle]$$

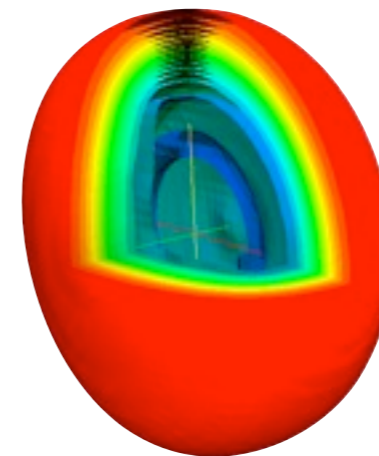
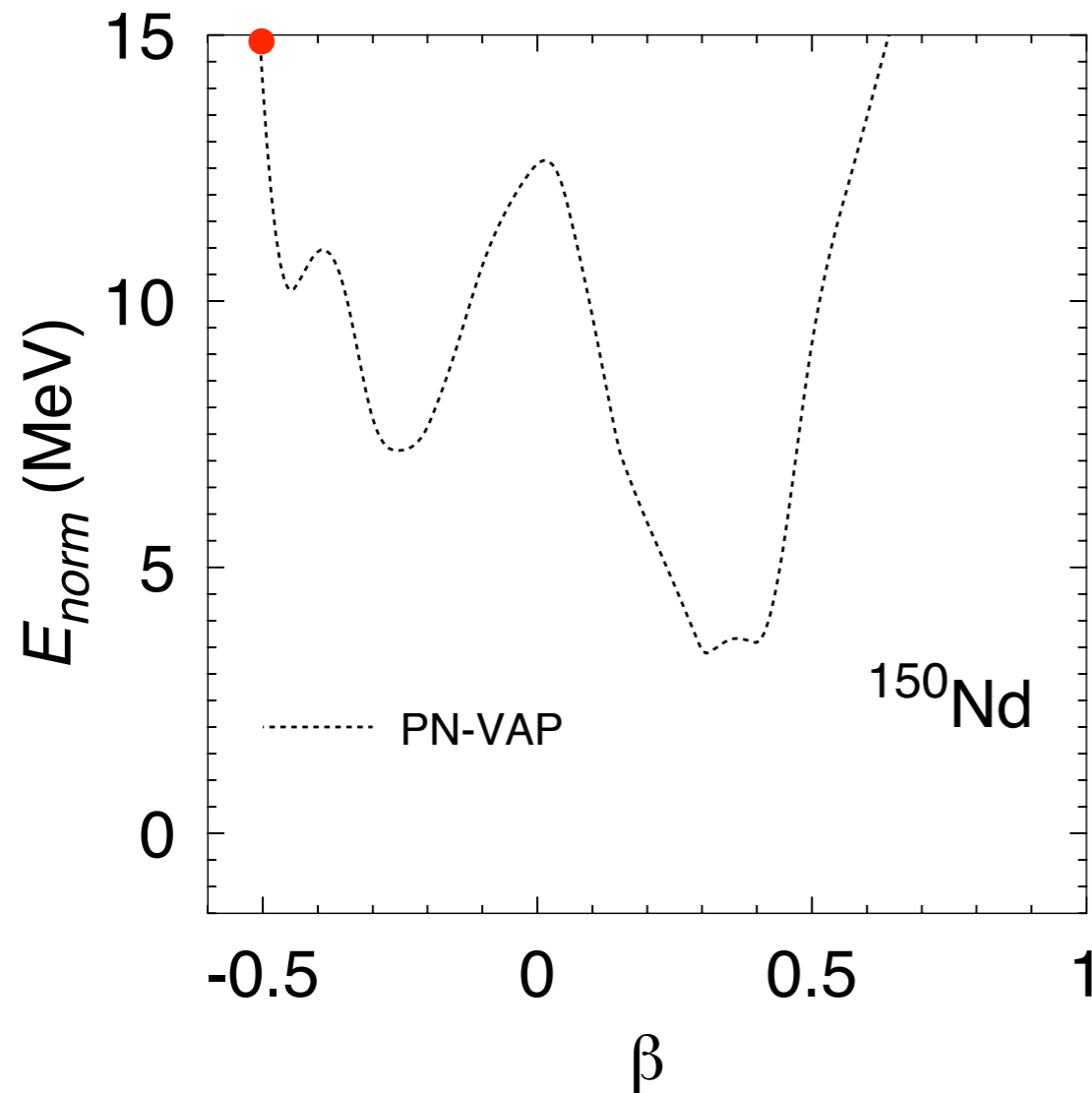
→ generalized eigenvalue problem

Particle number projection

Determination of initial and final states (I)

$$|\Phi\rangle \text{ HFB states} \longrightarrow \delta \left(E^{N,Z} [|\bar{\Phi}(q)\rangle] \right)_{|\bar{\Phi}\rangle=|\Phi\rangle} = 0$$

$$E^{N,Z}[|\Phi\rangle] = \frac{\langle \Phi | \hat{H} \hat{P}^N \hat{P}^Z | \Phi \rangle}{\langle \Phi | \hat{P}^N \hat{P}^Z | \Phi \rangle} + \varepsilon_{DD}^{N,Z}(|\Phi\rangle) - \lambda_q \langle \Phi | \hat{Q} | \Phi \rangle$$

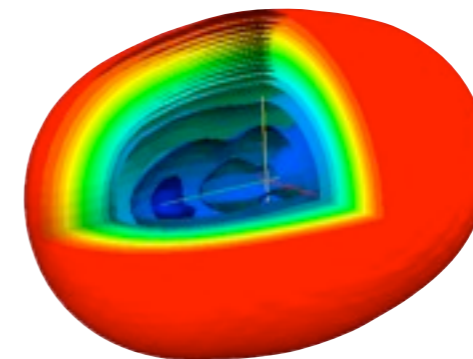
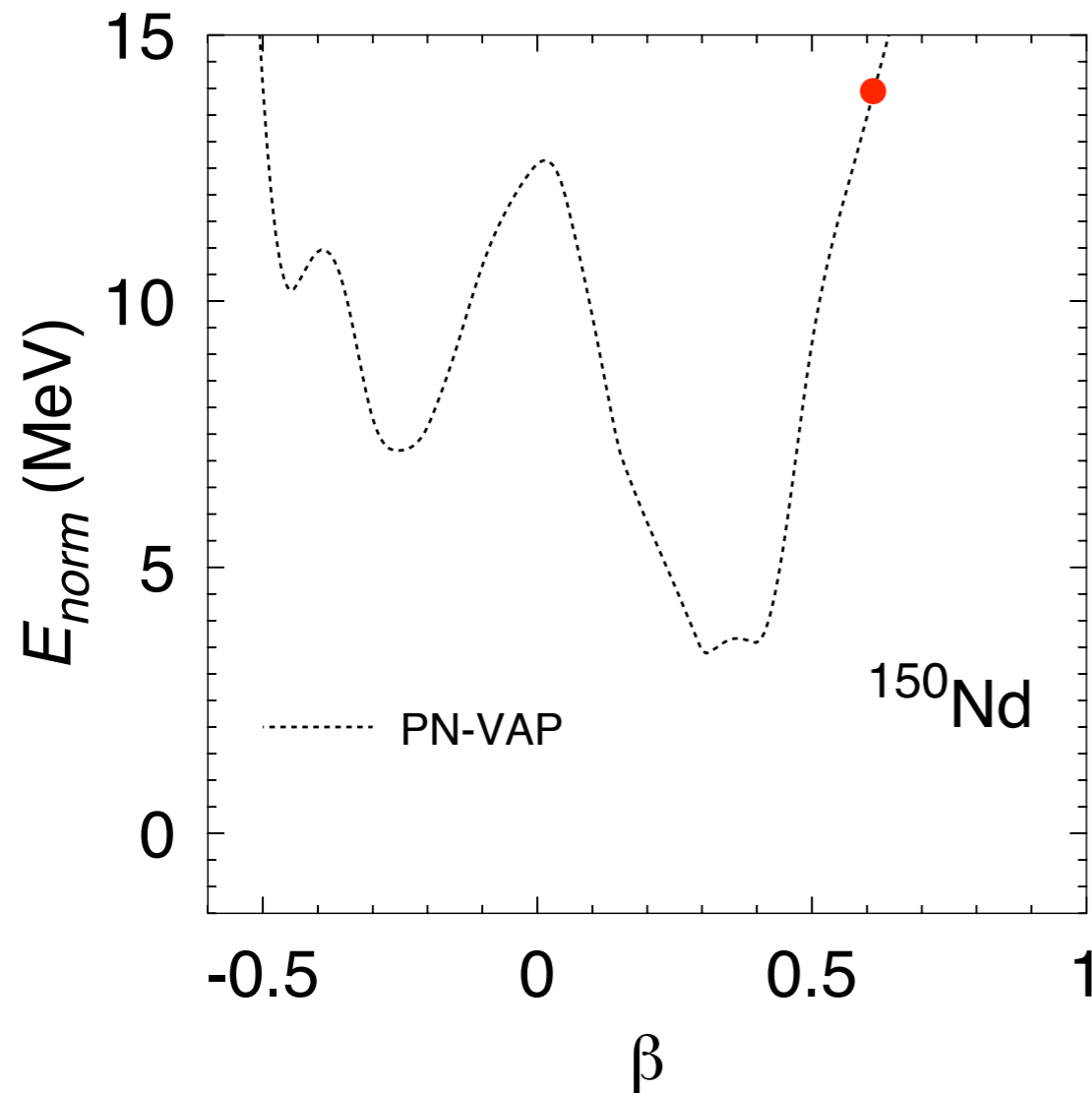


Particle number projection

Determination of initial and final states (I)

$$|\Phi\rangle \text{ HFB states} \longrightarrow \delta \left(E^{N,Z} [|\bar{\Phi}(q)\rangle] \right)_{|\bar{\Phi}\rangle=|\Phi\rangle} = 0$$

$$E^{N,Z}[|\Phi\rangle] = \frac{\langle \Phi | \hat{H} \hat{P}^N \hat{P}^Z | \Phi \rangle}{\langle \Phi | \hat{P}^N \hat{P}^Z | \Phi \rangle} + \varepsilon_{DD}^{N,Z}(|\Phi\rangle) - \lambda_q \langle \Phi | \hat{Q} | \Phi \rangle$$

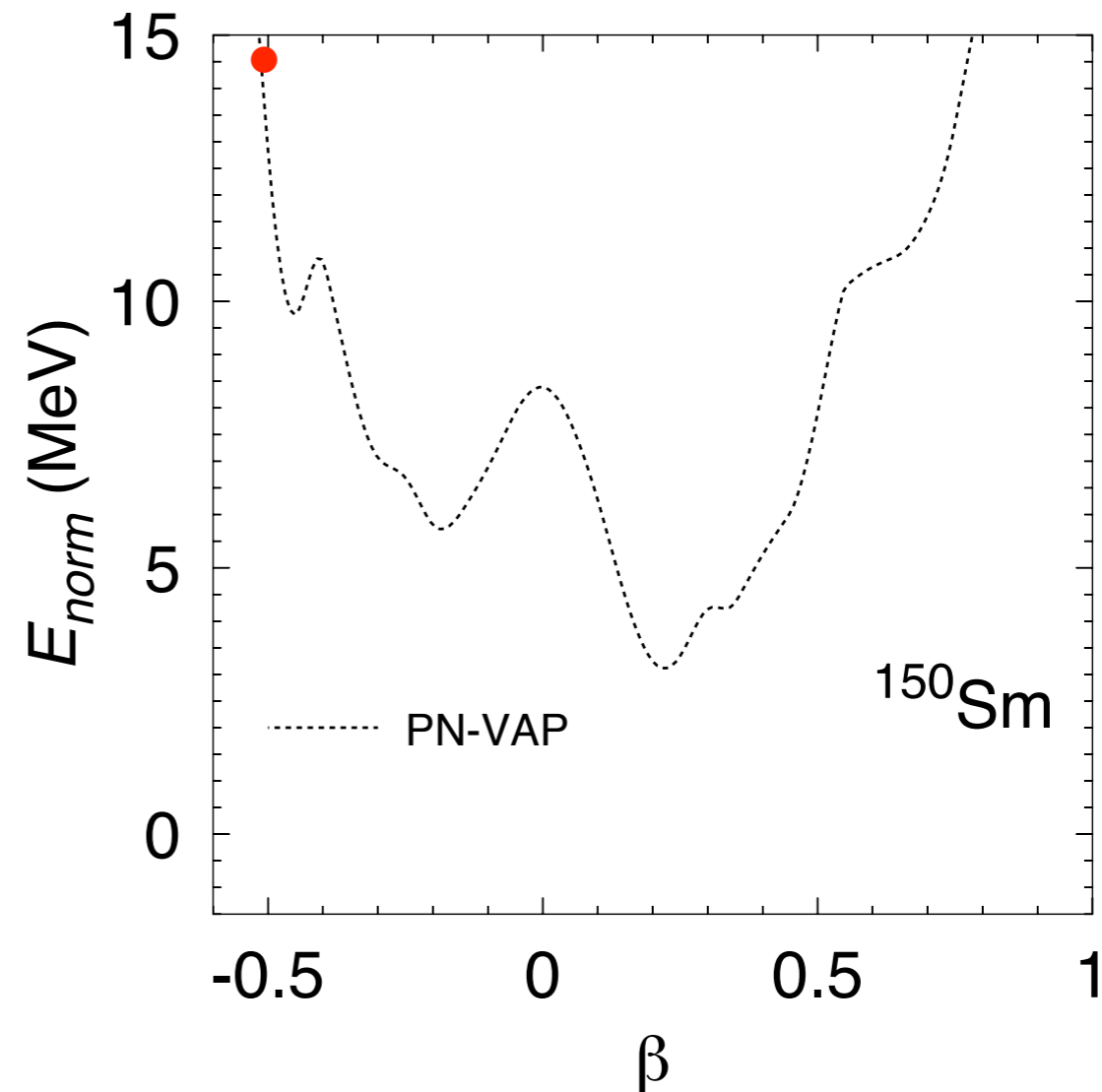
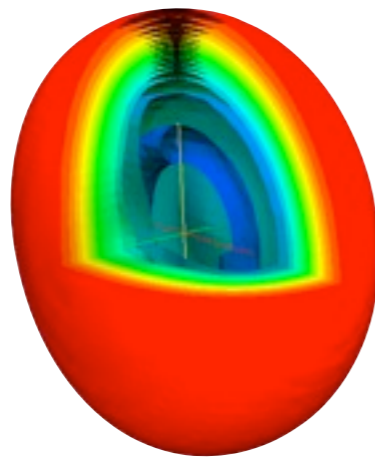


Particle number projection

Determination of initial and final states (I)

$$|\Phi\rangle \text{ HFB states} \longrightarrow \delta(E^{N,Z} [|\bar{\Phi}(q)\rangle])_{|\bar{\Phi}\rangle=|\Phi\rangle} = 0$$

$$E^{N,Z}[|\Phi\rangle] = \frac{\langle \Phi | \hat{H} \hat{P}^N \hat{P}^Z | \Phi \rangle}{\langle \Phi | \hat{P}^N \hat{P}^Z | \Phi \rangle} + \varepsilon_{DD}^{N,Z}(|\Phi\rangle) - \lambda_q \langle \Phi | \hat{Q} | \Phi \rangle$$

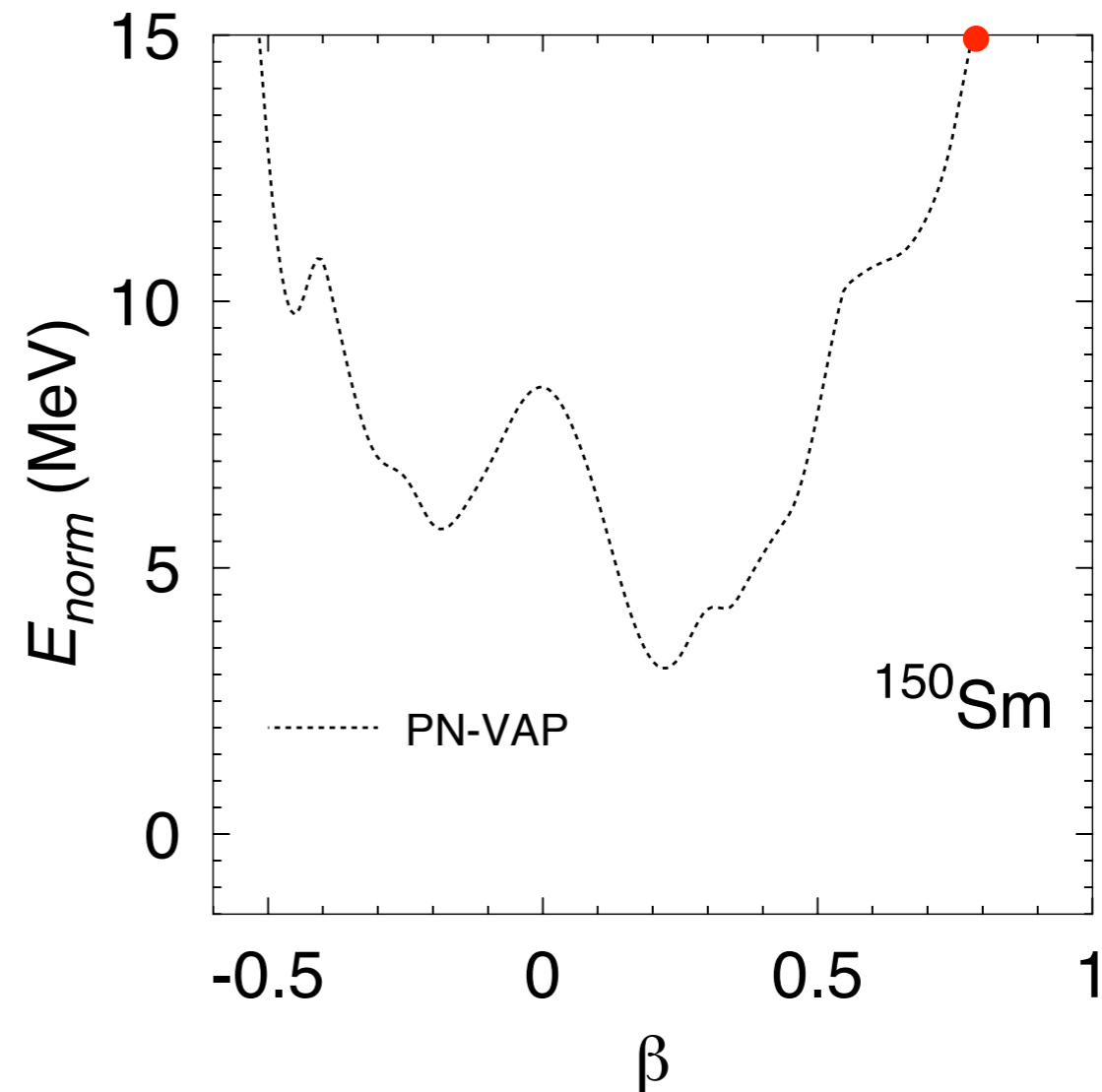
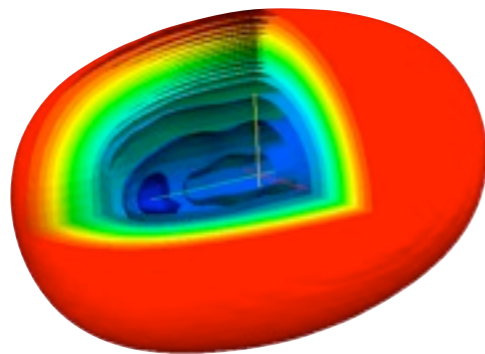


Particle number projection

Determination of initial and final states (I)

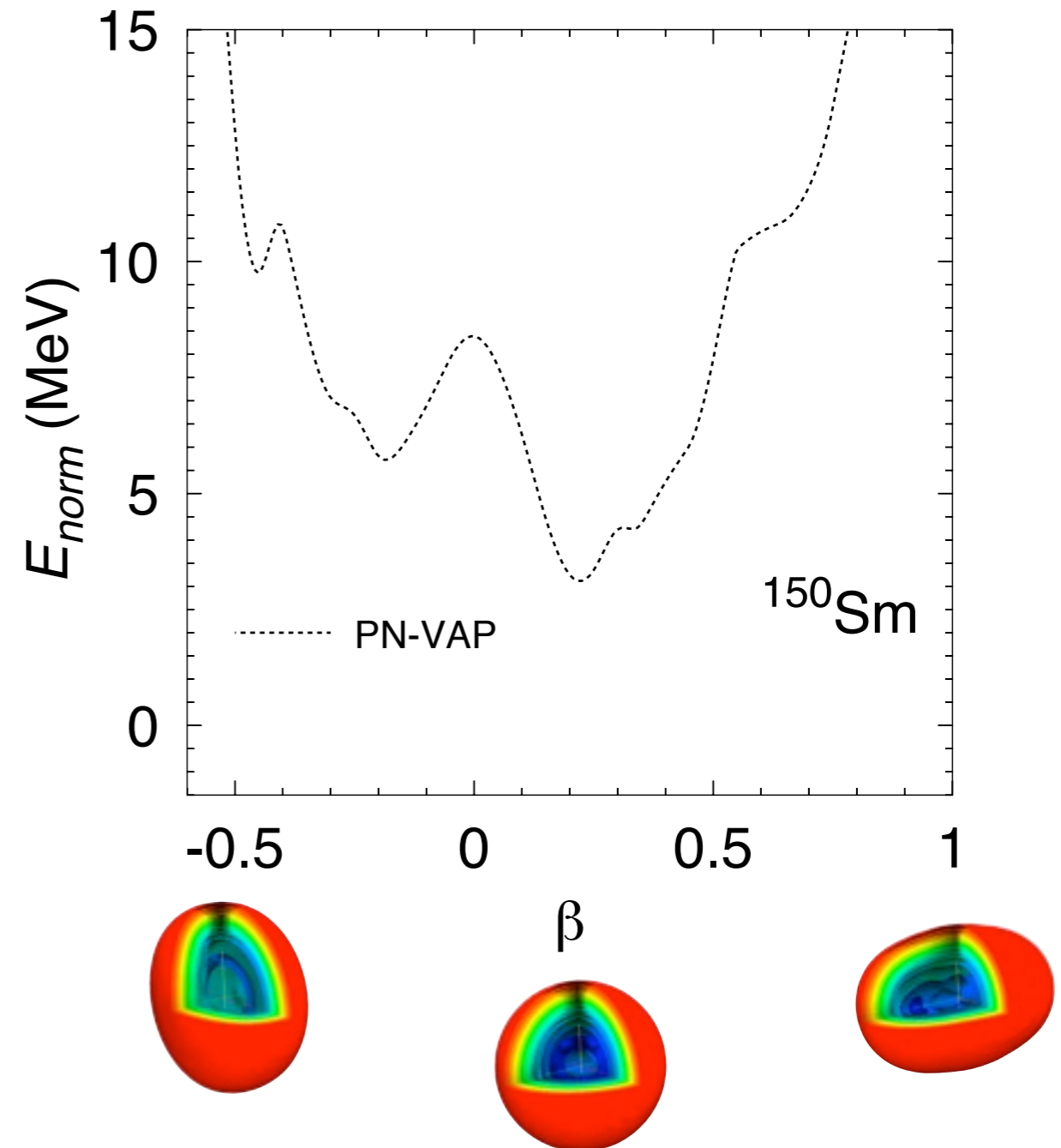
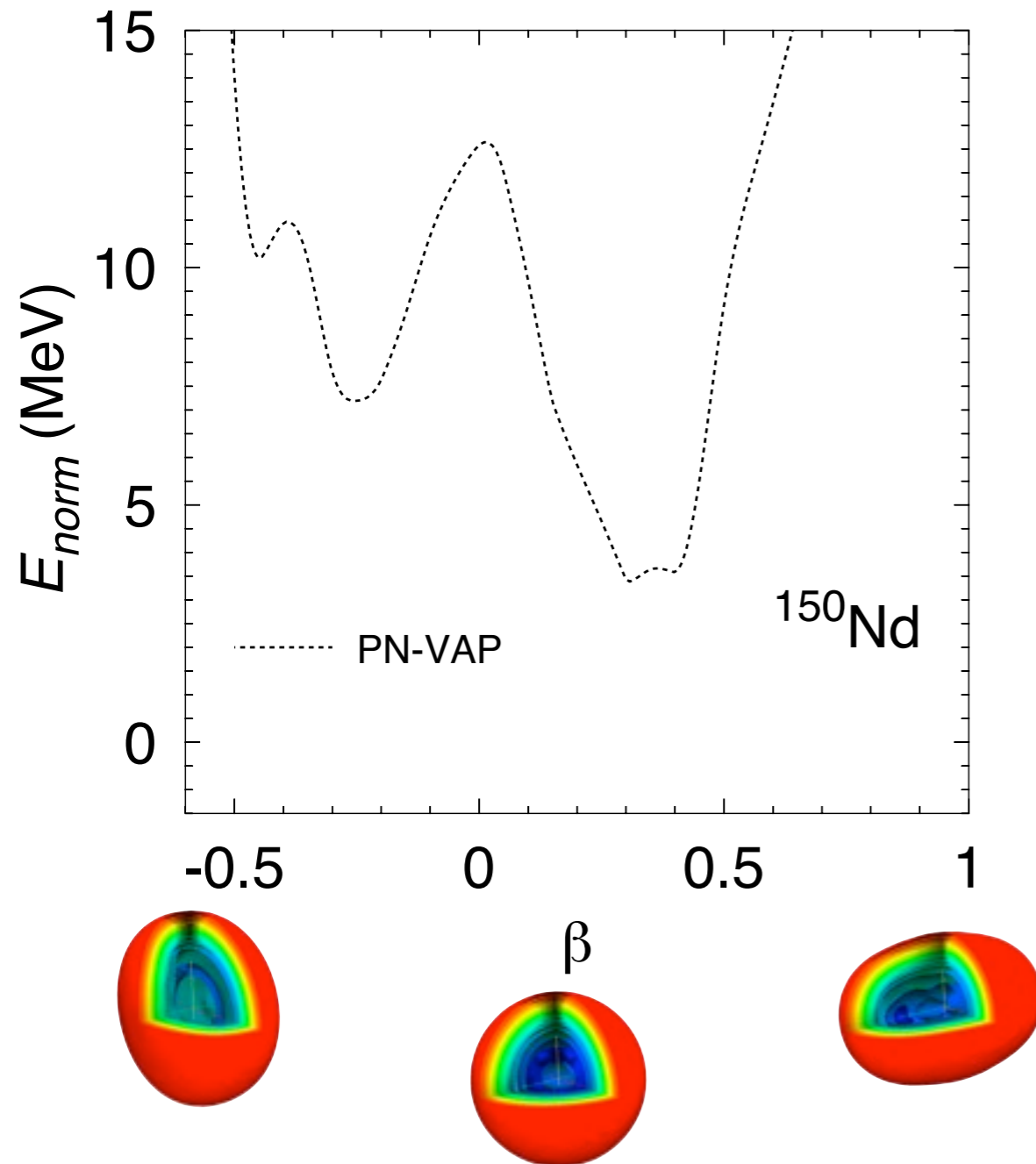
$$|\Phi\rangle \text{ HFB states} \longrightarrow \delta(E^{N,Z} [|\bar{\Phi}(q)\rangle])_{|\bar{\Phi}\rangle=|\Phi\rangle} = 0$$

$$E^{N,Z}[|\Phi\rangle] = \frac{\langle\Phi|\hat{H}\hat{P}^N\hat{P}^Z|\Phi\rangle}{\langle\Phi|\hat{P}^N\hat{P}^Z|\Phi\rangle} + \varepsilon_{DD}^{N,Z}(|\Phi\rangle) - \lambda_q \langle\Phi|\hat{Q}|\Phi\rangle$$



Particle number projection

Determination of initial and final states (I)



Particle number and angular momentum projection

Determination of initial and final states (II)

Intrinsic state: Solve the PN-VAP equations with the Gogny DIS interaction

$$|\Phi\rangle \text{ HFB states} \longrightarrow \delta \left(E^{N,Z} [|\bar{\Phi}(q)\rangle] \right)_{|\bar{\Phi}\rangle=|\Phi\rangle} = 0$$

$$E^{N,Z} [|\Phi\rangle] = \frac{\langle \Phi | \hat{H} \hat{P}^N \hat{P}^Z | \Phi \rangle}{\langle \Phi | \hat{P}^N \hat{P}^Z | \Phi \rangle} + \varepsilon_{DD}^{N,Z} (|\Phi\rangle) - \lambda_q \langle \Phi | \hat{Q} | \Phi \rangle$$

Particle number and angular momentum projected state:

$$|IMK; NZ; q\rangle = \frac{2I+1}{8\pi^2} \int \mathcal{D}_{MK}^{I*}(\Omega) \hat{R}(\Omega) \hat{P}^N \hat{P}^Z |\Phi(q)\rangle d\Omega$$

General form (GCM state):

$$|IM; NZ\sigma\rangle = \sum_{Kq} f_{Kq}^{I;NZ,\sigma} |IMK; NZ; q\rangle$$

Hill-Wheeler-Griffin equation (GCM)

$$\sum_{K'q'} \left(\mathcal{H}_{KqK'q'}^{I;NZ} - E^{I;NZ;\sigma} \mathcal{N}_{KqK'q'}^{I;NZ} \right) f_{K'q'}^{I;NZ;\sigma} = 0$$

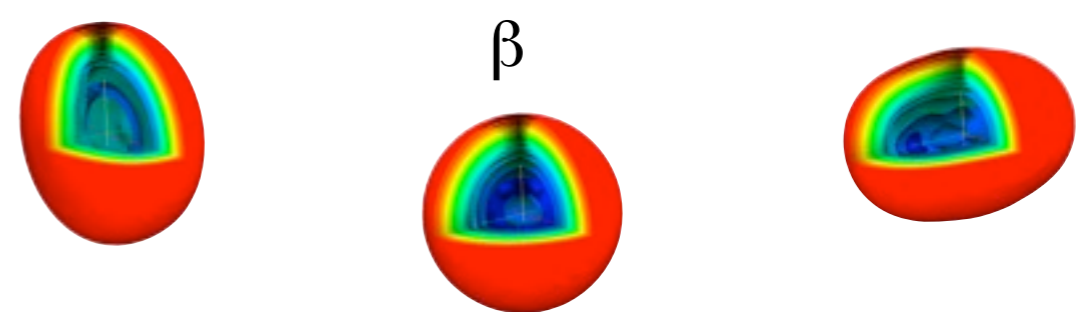
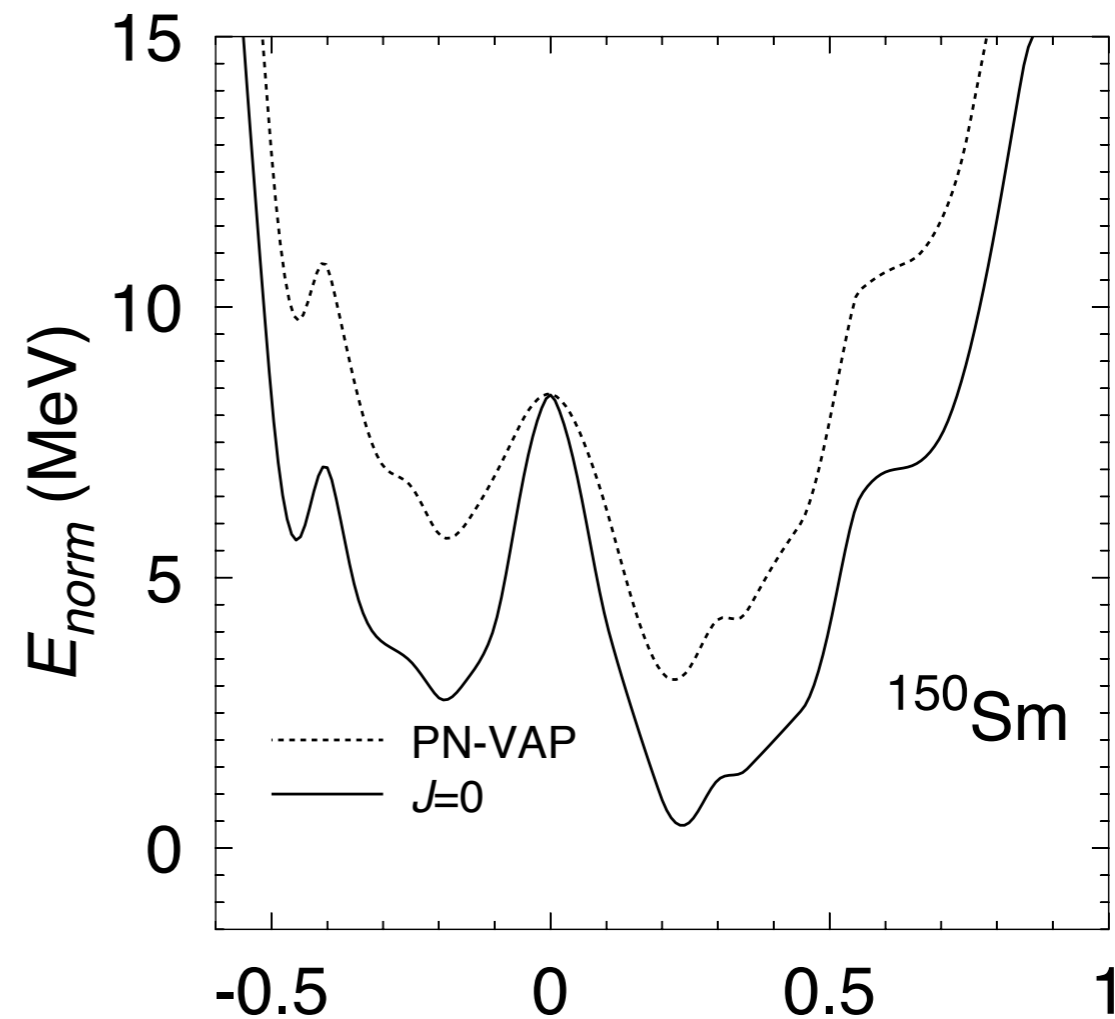
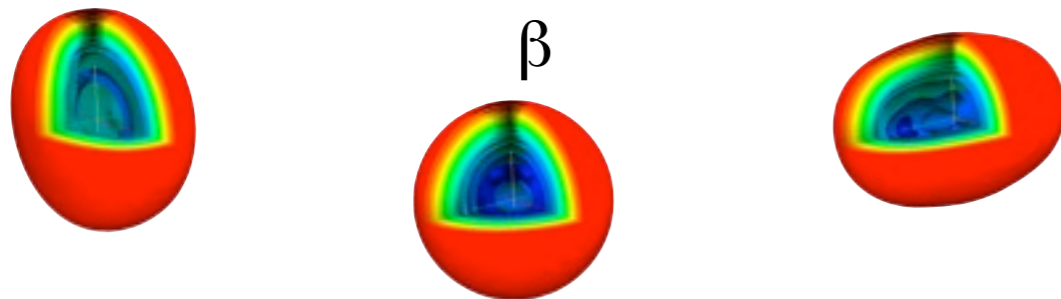
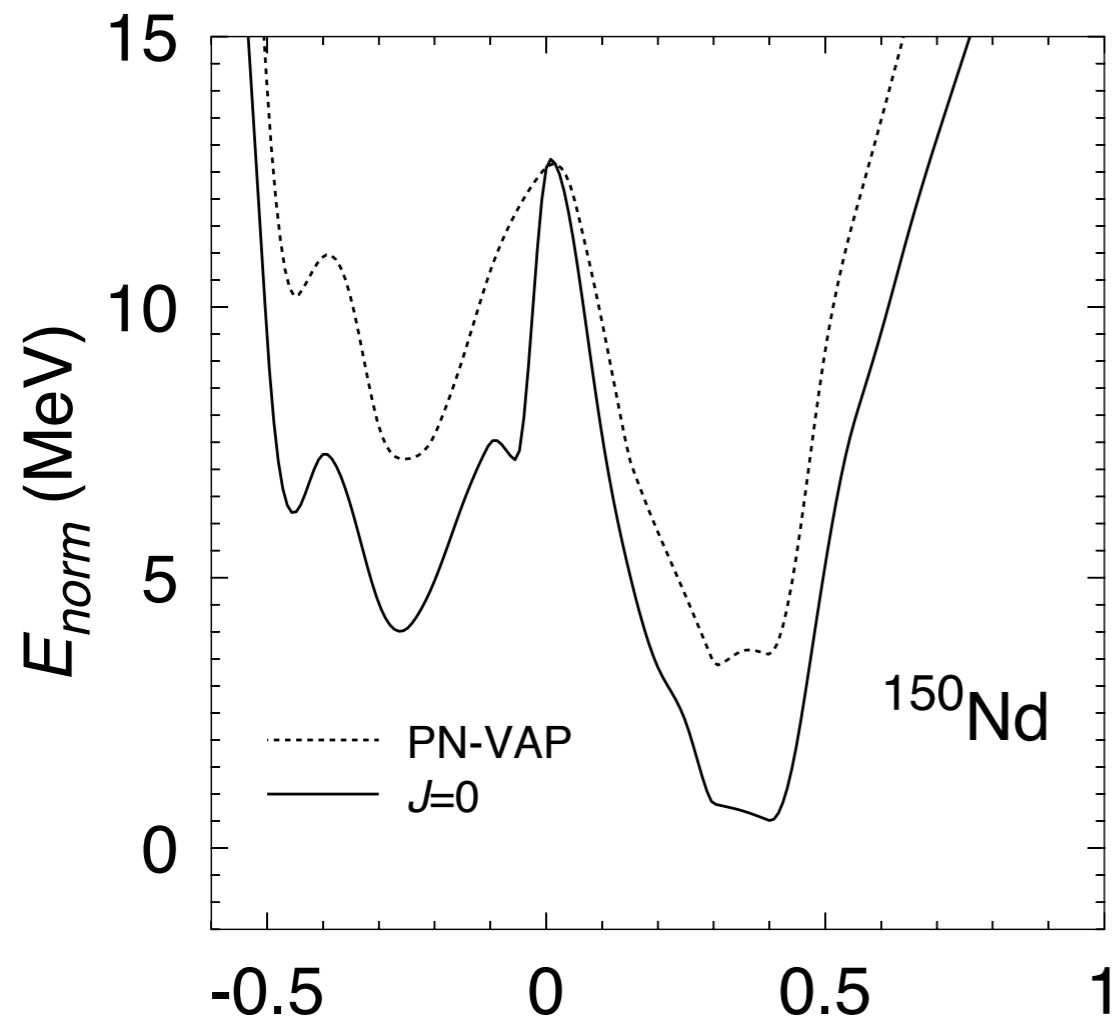
$$\mathcal{N}_{KqK'q'}^{I;NZ} \equiv \langle IMK; NZ; q | IMK'; NZ; q' \rangle$$

$$\mathcal{H}_{KqK'q'}^{I;NZ} \equiv \langle IMK; NZ; q | \hat{H} | IMK'; NZ; q' \rangle + \varepsilon_{DD}^{IKK';NZ} [|\Phi(q)\rangle, |\Phi(q')\rangle]$$

→ generalized eigenvalue problem

Particle number and angular momentum projection

Determination of initial and final states (II)



Configuration (shape) mixing

Determination of initial and final states (& III)

Intrinsic state: Solve the PN-VAP equations with the Gogny DIS interaction

$$|\Phi\rangle \text{ HFB states} \longrightarrow \delta (E^{N,Z} [|\bar{\Phi}(q)\rangle])_{|\bar{\Phi}\rangle=|\Phi\rangle} = 0$$

$$E^{N,Z} [|\Phi\rangle] = \frac{\langle \Phi | \hat{H} \hat{P}^N \hat{P}^Z | \Phi \rangle}{\langle \Phi | \hat{P}^N \hat{P}^Z | \Phi \rangle} + \varepsilon_{DD}^{N,Z} (|\Phi\rangle) - \lambda_q \langle \Phi | \hat{Q} | \Phi \rangle$$

Particle number and angular momentum projected state:

$$|IMK; NZ; q\rangle = \frac{2I+1}{8\pi^2} \int \mathcal{D}_{MK}^{I*}(\Omega) \hat{R}(\Omega) \hat{P}^N \hat{P}^Z |\Phi(q)\rangle d\Omega$$

General form (GCM state):

$$|IM; NZ\sigma\rangle = \sum_{Kq} f_{Kq}^{I;NZ,\sigma} |IMK; NZ; q\rangle$$

$$\sum_{K'q'} \left(\mathcal{H}_{KqK'q'}^{I;NZ} - E^{I;NZ;\sigma} \mathcal{N}_{KqK'q'}^{I;NZ} \right) f_{K'q'}^{I;NZ;\sigma} = 0$$

Hill-Wheeler-Griffin equation (GCM)

$$\mathcal{N}_{KqK'q'}^{I;NZ} \equiv \langle IMK; NZ; q | IMK'; NZ; q' \rangle$$

$$\mathcal{H}_{KqK'q'}^{I;NZ} \equiv \langle IMK; NZ; q | \hat{H} | IMK'; NZ; q' \rangle + \varepsilon_{DD}^{IKK';NZ} [|\Phi(q)\rangle, |\Phi(q')\rangle]$$

—————> generalized eigenvalue problem

Configuration (shape) mixing

Determination of initial and final states (& III)

Intrinsic state: Solve the PN-VAP equations with the Gogny DIS interaction

$$|\Phi\rangle \text{ HFB states } \longrightarrow \delta \left(E^{N,Z} [|\bar{\Phi}(q)\rangle] \right)_{|\bar{\Phi}\rangle=|\Phi\rangle} = 0$$

$$E^{N,Z} [|\Phi\rangle] = \frac{\langle \Phi | \hat{H} \hat{P}^N \hat{P}^Z | \Phi \rangle}{\langle \Phi | \hat{P}^N \hat{P}^Z | \Phi \rangle} + \varepsilon_{DD}^{N,Z} (|\Phi\rangle) - \lambda_q \langle \Phi | \hat{Q} | \Phi \rangle$$

Particle number and angular momentum projected state:

$$|IMK; NZ; q\rangle = \frac{2I+1}{8\pi^2} \int \mathcal{D}_{MK}^{I*}(\Omega) \hat{R}(\Omega) \hat{P}^N \hat{P}^Z |\Phi(q)\rangle d\Omega$$

General form (GCM state):

$$|IM; NZ\sigma\rangle = \sum_{Kq} f_{Kq}^{I;NZ,\sigma} |IMK; NZ; q\rangle$$

Solving HWG equation:

1. Diagonalization of the norm overlap:

$$\sum_{K'q'} \mathcal{N}_{KqK'q'}^{I;NZ} u_{K'q';\Lambda}^{I;NZ} = n_{\Lambda}^{I;NZ} u_{Kq;\Lambda}^{I;NZ}$$

2. Natural basis:

$$|\Lambda^{IM;NZ}\rangle = \sum_{Kq} \frac{u_{Kq;\Lambda}^{I;NZ}}{\sqrt{n_{\Lambda}^{I;NZ}}} |IMK; NZ; q\rangle ; n_{\Lambda}^{I;NZ} / n_{max}^{I;NZ} > \zeta$$

3. Normal eigenvalue problem:

$$\sum_{\Lambda'} \langle \Lambda^{I;NZ} | \hat{H} | \Lambda'^{I;NZ} \rangle G_{\Lambda'}^{I;NZ;\sigma} = E^{I;NZ;\sigma} G_{\Lambda}^{I;NZ;\sigma}$$

Configuration (shape) mixing

Determination of initial and final states (& III)

Intrinsic state: Solve the PN-VAP equations with the Gogny DIS interaction

$$|\Phi\rangle \text{ HFB states } \longrightarrow \delta \left(E^{N,Z} [|\bar{\Phi}(q)\rangle] \right)_{|\bar{\Phi}\rangle=|\Phi\rangle} = 0$$

$$E^{N,Z} [|\Phi\rangle] = \frac{\langle \Phi | \hat{H} \hat{P}^N \hat{P}^Z | \Phi \rangle}{\langle \Phi | \hat{P}^N \hat{P}^Z | \Phi \rangle} + \varepsilon_{DD}^{N,Z} (|\Phi\rangle) - \lambda_q \langle \Phi | \hat{Q} | \Phi \rangle$$

Particle number and angular momentum projected state:

$$|IMK; NZ; q\rangle = \frac{2I+1}{8\pi^2} \int \mathcal{D}_{MK}^{I*}(\Omega) \hat{R}(\Omega) \hat{P}^N \hat{P}^Z |\Phi(q)\rangle d\Omega$$

General form (GCM state):

$$|IM; NZ\sigma\rangle = \sum_{\Lambda} G_{\Lambda}^{I;NZ;\sigma} |\Lambda^{I;NZ}\rangle$$

Solving HWG equation:

1. Diagonalization of the norm overlap:

$$\sum_{K'q'} \mathcal{N}_{KqK'q'}^{I;NZ} u_{K'q';\Lambda}^{I;NZ} = n_{\Lambda}^{I;NZ} u_{Kq;\Lambda}^{I;NZ}$$

2. Natural basis:

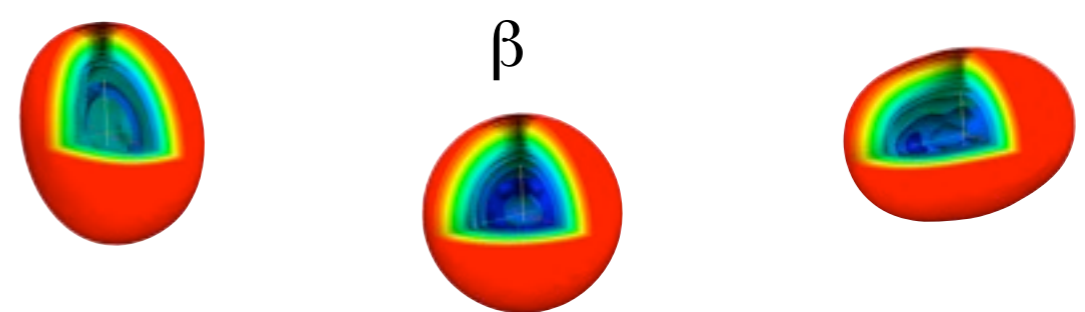
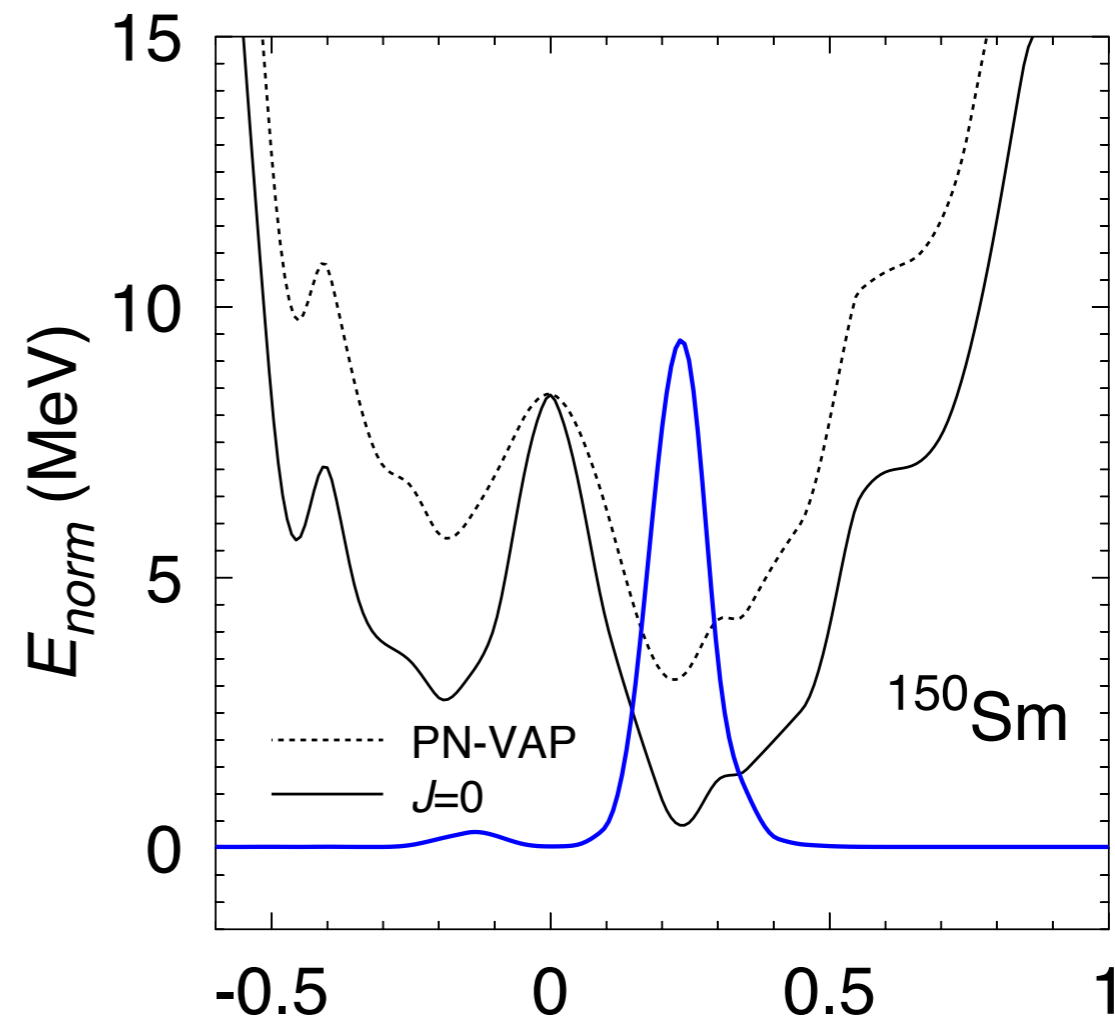
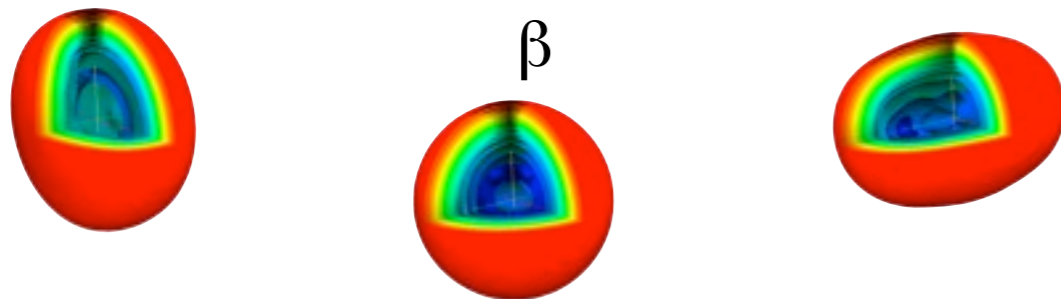
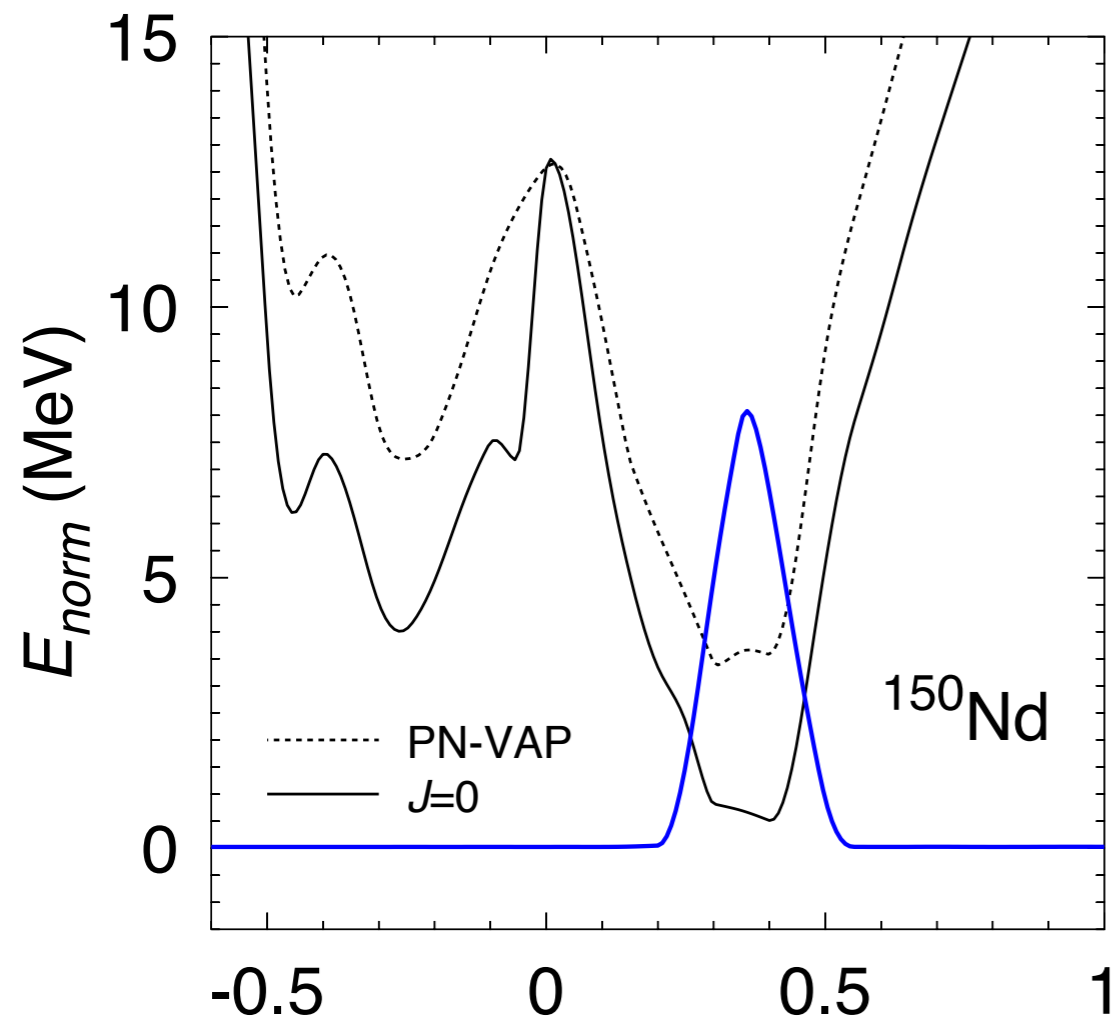
$$|\Lambda^{IM;NZ}\rangle = \sum_{Kq} \frac{u_{Kq;\Lambda}^{I;NZ}}{\sqrt{n_{\Lambda}^{I;NZ}}} |IMK; NZ; q\rangle ; n_{\Lambda}^{I;NZ} / n_{max}^{I;NZ} > \zeta$$

3. Normal eigenvalue problem:

$$\sum_{\Lambda'} \langle \Lambda^{I;NZ} | \hat{H} | \Lambda'^{I;NZ} \rangle G_{\Lambda'}^{I;NZ;\sigma} = E^{I;NZ;\sigma} G_{\Lambda}^{I;NZ;\sigma}$$

Configuration (shape) mixing

Determination of initial and final states (& III)



Transitions

1. Axial states $K = 0$
2. Angular momentum $I = 0$
3. Quadrupole deformations $q = q_{20}$



$$\begin{aligned} |0; N_i Z_i; \sigma\rangle &= \sum_{\Lambda_i} G_{\Lambda_i}^{0; N_i Z_i; \sigma} |\Lambda_i^{0; N_i Z_i}\rangle \\ |0; N_f Z_f; \sigma\rangle &= \sum_{\Lambda_f} G_{\Lambda_f}^{0; N_f Z_f; \sigma} |\Lambda_f^{0; N_f Z_f}\rangle \end{aligned}$$

Transitions

1. Axial states $K = 0$
2. Angular momentum $I = 0$
3. Quadrupole deformations $q = q_{20}$



$$|0; N_i Z_i; \sigma\rangle = \sum_{\Lambda_i} G_{\Lambda_i}^{0; N_i Z_i; \sigma} |\Lambda_i^{0; N_i Z_i}\rangle$$

$$|0; N_f Z_f; \sigma\rangle = \sum_{\Lambda_f} G_{\Lambda_f}^{0; N_f Z_f; \sigma} |\Lambda_f^{0; N_f Z_f}\rangle$$

TRANSITIONS:

$$M_{\xi}^{0\nu\beta\beta} = \langle 0_f^+ | \hat{O}_{\xi}^{0\nu\beta\beta} | 0_i^+ \rangle = \langle 0; N_f Z_f | \hat{O}_{\xi}^{0\nu\beta\beta} | 0; N_i Z_i \rangle =$$

$$\sum_{\Lambda_f \Lambda_i} \left(G_{\Lambda_f}^{0; N_f Z_f} \right)^* \langle \Lambda_f^{0; N_f Z_f} | \hat{O}_{\xi}^{0\nu\beta\beta} | \Lambda_i^{0; N_i Z_i} \rangle G_{\Lambda_i}^{0; N_i Z_i} = \sum_{q_i q_f; \Lambda_f \Lambda_i}$$

$$\left(\frac{u_{q_f, \Lambda_f}^{0; N_f Z_f}}{\sqrt{n_{\Lambda_f}^{0; N_f Z_f}}} \right)^* \left(G_{\Lambda_f}^{0; N_f Z_f} \right)^* \langle 0; N_f Z_f; q_f | \hat{O}_{\xi}^{0\nu\beta\beta} | 0; N_i Z_i; q_i \rangle \left(G_{\Lambda_i}^{0; N_i Z_i} \right) \left(\frac{u_{q_i, \Lambda_i}^{0; N_i Z_i}}{\sqrt{n_{\Lambda_i}^{0; N_i Z_i}}} \right)$$

Transitions

1. Axial states $K = 0$
2. Angular momentum $I = 0$
3. Quadrupole deformations $q = q_{20}$



$$|0; N_i Z_i; \sigma\rangle = \sum_{\Lambda_i} G_{\Lambda_i}^{0; N_i Z_i; \sigma} |\Lambda_i^{0; N_i Z_i}\rangle$$

$$|0; N_f Z_f; \sigma\rangle = \sum_{\Lambda_f} G_{\Lambda_f}^{0; N_f Z_f; \sigma} |\Lambda_f^{0; N_f Z_f}\rangle$$

TRANSITIONS:

$$M_{\xi}^{0\nu\beta\beta} = \langle 0_f^+ | \hat{O}_{\xi}^{0\nu\beta\beta} | 0_i^+ \rangle = \langle 0; N_f Z_f | \hat{O}_{\xi}^{0\nu\beta\beta} | 0; N_i Z_i \rangle =$$

$$\sum_{\Lambda_f \Lambda_i} \left(G_{\Lambda_f}^{0; N_f Z_f} \right)^* \langle \Lambda_f^{0; N_f Z_f} | \hat{O}_{\xi}^{0\nu\beta\beta} | \Lambda_i^{0; N_i Z_i} \rangle G_{\Lambda_i}^{0; N_i Z_i} = \sum_{q_i q_f; \Lambda_f \Lambda_i}$$

$$\left(\frac{u_{q_f, \Lambda_f}^{0; N_f Z_f}}{\sqrt{n_{\Lambda_f}^{0; N_f Z_f}}} \right)^* \left(G_{\Lambda_f}^{0; N_f Z_f} \right)^* \langle 0; N_f Z_f; q_f | \hat{O}_{\xi}^{0\nu\beta\beta} | 0; N_i Z_i; q_i \rangle \left(G_{\Lambda_i}^{0; N_i Z_i} \right) \left(\frac{u_{q_i, \Lambda_i}^{0; N_i Z_i}}{\sqrt{n_{\Lambda_i}^{0; N_i Z_i}}} \right)$$

Matrix elements of the double beta transition operators between particle number and angular momentum projected states

Nuclear structure properties

Neutrinoless double beta decay candidates

440

T.R. Rodríguez, G. Martínez-Pinedo / Progress in Particle and Nuclear Physics 66 (2011) 436–440

Table 1

Masses, rms charge radii and total Gamow–Teller strengths $S_{-(+)}$ for mother (granddaughter) calculated with Gogny D1S GCM+PNAMP functional compared to experimental values. Theoretical values for $S_{+/-}$ are quenched by a factor $(0.74)^2$.

Isotope	BE_{th} (MeV)	BE^{exp} (MeV) [27]	R_{th} (fm)	R^{exp} (fm) [28]	$S_{-/+}^{theo}$	$S_{-/+}^{exp}$
^{48}Ca	420.623	415.991	3.465	3.473	13.55	(14.4 ± 2.2 [29])
^{48}Ti	423.597	418.699	3.557	3.591	1.99	(1.9 ± 0.5 [29])
^{76}Ge	664.204	661.598	4.024	4.081	20.97	(19.89 [30])
^{76}Se	664.949	662.072	4.074	4.139	1.49	(1.45 ± 0.07 [31])
^{82}Se	716.794	712.842	4.100	4.139	23.56	(21.91 [30])
^{82}Kr	717.859	714.273	4.130	4.192	1.24	
^{96}Zr	829.432	828.995	4.298	4.349	27.63	
^{96}Mo	833.793	830.778	4.319	4.384	2.56	(0.29 ± 0.08 [32])
^{100}Mo	861.526	860.457	4.372	4.445	27.87	(26.69 [30])
^{100}Ru	864.875	861.927	4.388	4.453	2.48	
^{116}Cd	988.469	987.440	4.556	4.628	34.30	(32.70 [30])
^{116}Sn	991.079	988.684	4.567	4.626	2.61	(1.09 ^{+0.13} _{-0.57} [33])
^{124}Sn	1051.668	1049.96	4.622	4.675	40.65	
^{124}Te	1051.562	1050.69	4.664	4.717	1.63	
^{128}Te	1082.257	1081.44	4.686	4.735	40.48	(40.08 [30])
^{128}Xe	1080.996	1080.74	4.723	4.775	1.45	
^{130}Te	1096.627	1095.94	4.695	4.742	43.57	(45.90 [30])
^{130}Xe	1097.245	1096.91	4.732	4.783	1.19	
^{136}Xe	1143.333	1141.88	4.756	4.799	46.71	
^{136}Ba	1143.202	1142.77	4.786	4.832	0.96	
^{150}Nd	1234.512	1237.45	5.034	5.041	50.32	
^{150}Sm	1235.936	1239.25	5.041	5.040	1.45	

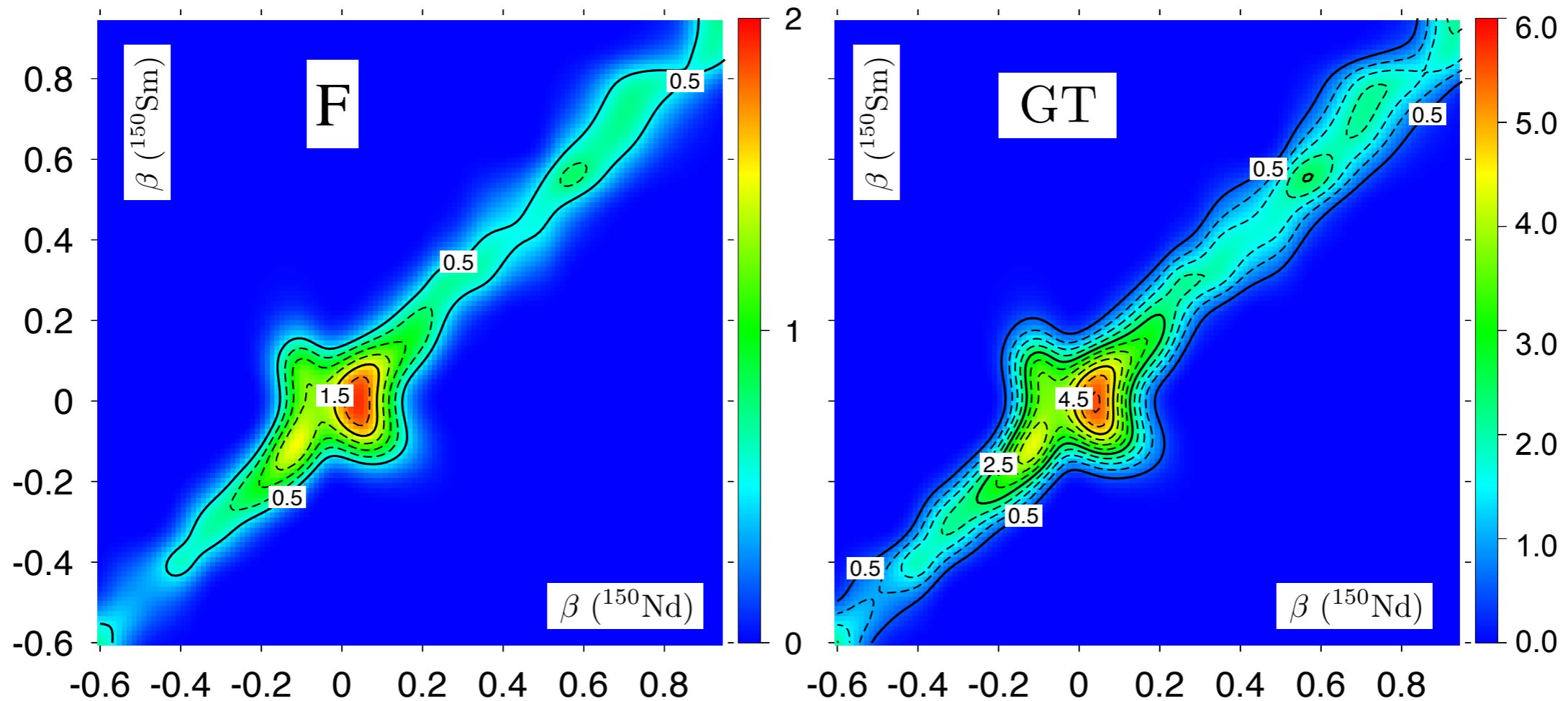
Good agreement between experimental and theoretical Q -values, radii and total strength (quenched)

NME: deformation and mixing

$$\frac{\langle 0; N_f Z_f; q_f | \hat{O}_\xi^{0\nu\beta\beta} | 0; N_i Z_i; q_i \rangle}{\sqrt{\langle 0; N_f Z_f; q_f | 0; N_f Z_f; q_f \rangle \langle 0; N_i Z_i; q_i | 0; N_i Z_i; q_i \rangle}}$$

A=150

T.R.R., Martínez-Pinedo, PRL 2010



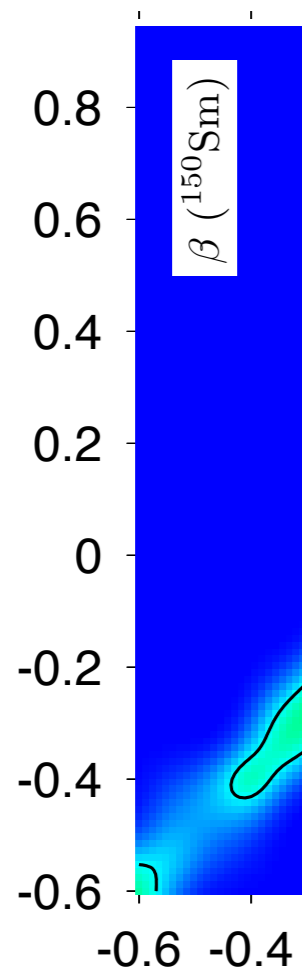
- GT strength greater than Fermi.
- Similar deformation between mother and granddaughter is favored by the transition operators
- Maxima are found close to sphericity although some other local maxima are found

NME: deformation and mixing

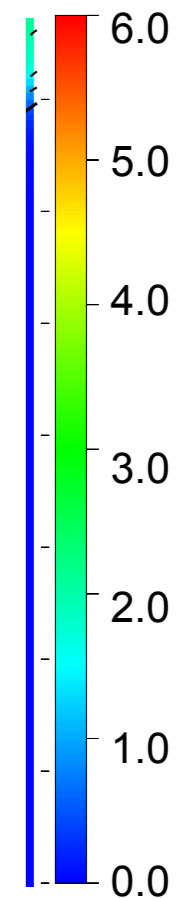
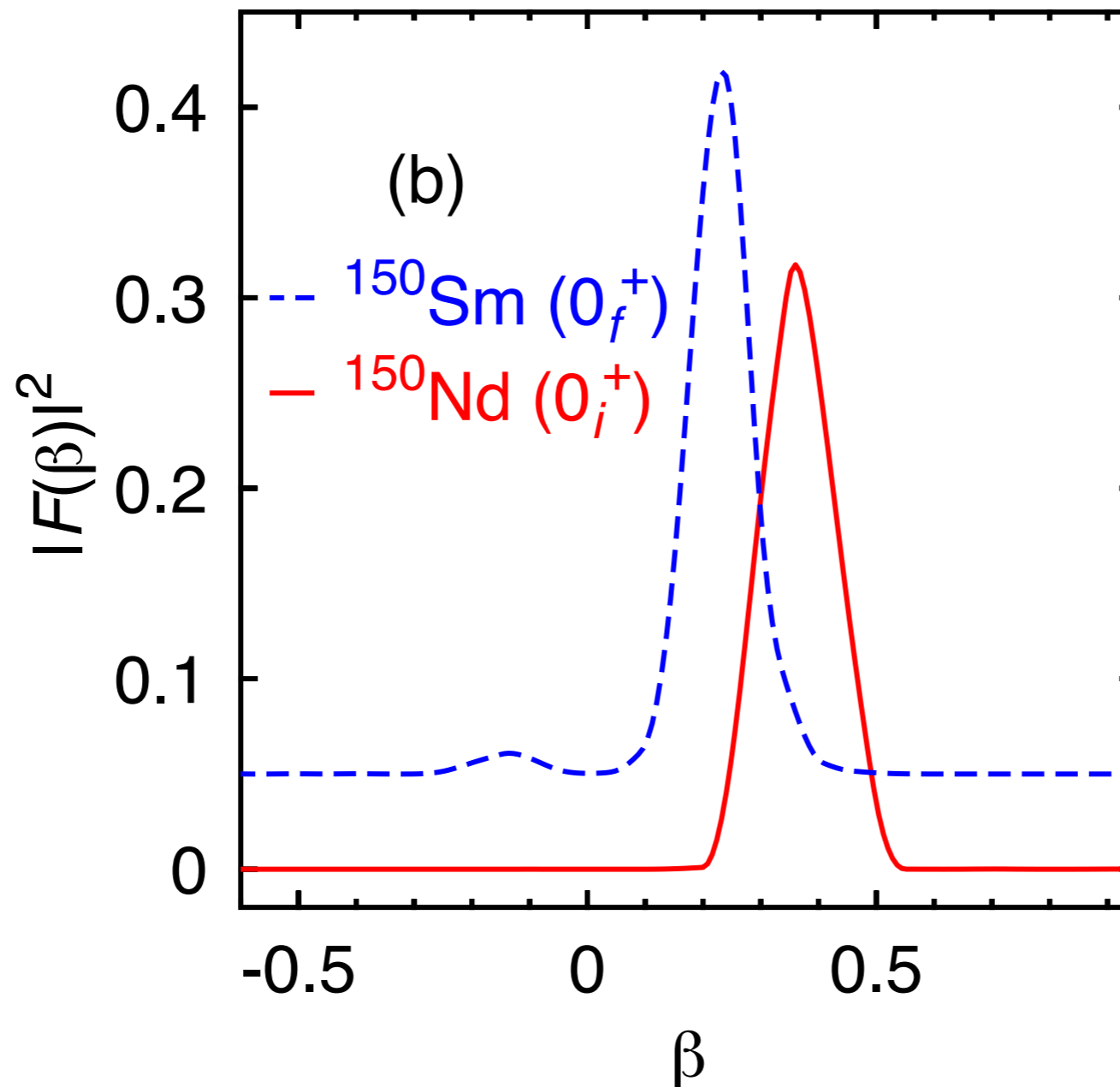
$$\frac{\langle 0; N_f Z_f; q_f | \hat{O}_\xi^{0\nu\beta\beta} | 0; N_i Z_i; q_i \rangle}{\sqrt{\langle 0; N_f Z_f; q_f | 0; N_f Z_f; q_f \rangle \langle 0; N_i Z_i; q_i | 0; N_i Z_i; q_i \rangle}}$$

A=150

T.R.R., Martínez-Pinedo, PRL 2010



- GT stren
- Similar de
- Maxima a
- Final resu
- states with...



rs

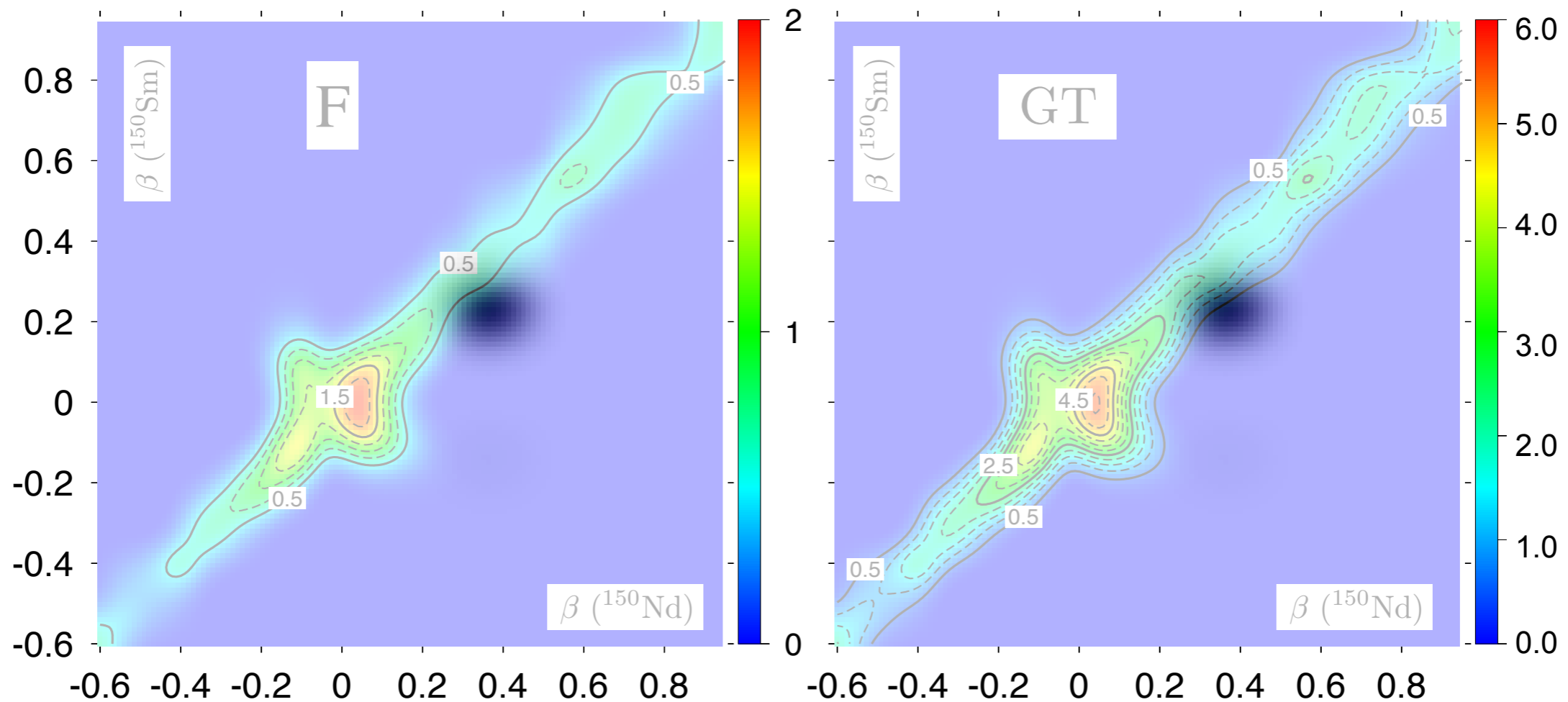
ollective

NME: deformation and mixing

$$\frac{\langle 0; N_f Z_f; q_f | \hat{O}_\xi^{0\nu\beta\beta} | 0; N_i Z_i; q_i \rangle}{\sqrt{\langle 0; N_f Z_f; q_f | 0; N_f Z_f; q_f \rangle \langle 0; N_i Z_i; q_i | 0; N_i Z_i; q_i \rangle}}$$

A=150

T.R.R., Martínez-Pinedo, PRL 2010



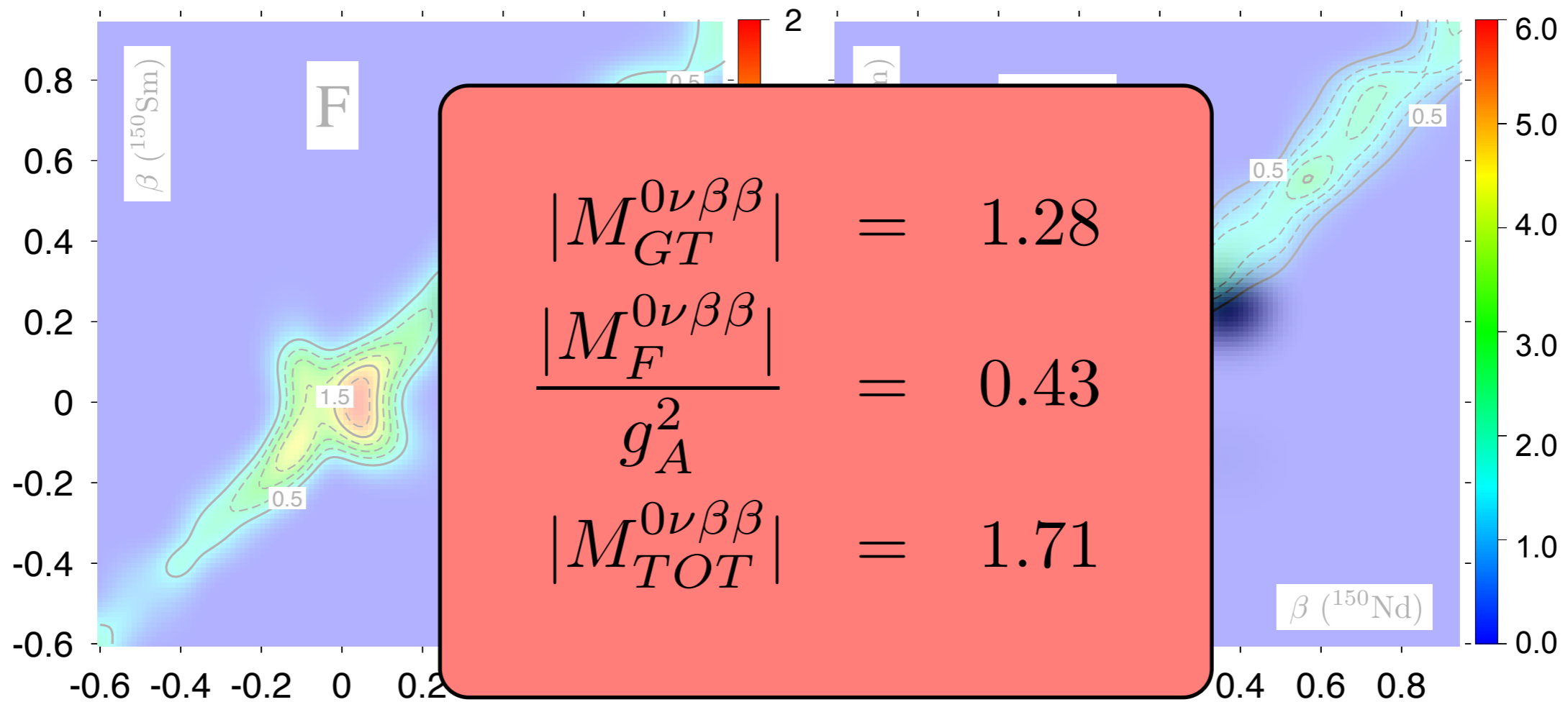
- GT strength greater than Fermi.
- Similar deformation between mother and granddaughter is favored by the transition operators
- Maxima are found close to sphericity although some other local maxima are found
- Final result depends on the distribution of probability of the corresponding initial and final collective states within this plot

NME: deformation and mixing

$$\frac{\langle 0; N_f Z_f; q_f | \hat{O}_\xi^{0\nu\beta\beta} | 0; N_i Z_i; q_i \rangle}{\sqrt{\langle 0; N_f Z_f; q_f | 0; N_f Z_f; q_f \rangle \langle 0; N_i Z_i; q_i | 0; N_i Z_i; q_i \rangle}}$$

A=150

T.R.R., Martínez-Pinedo, PRL 2010

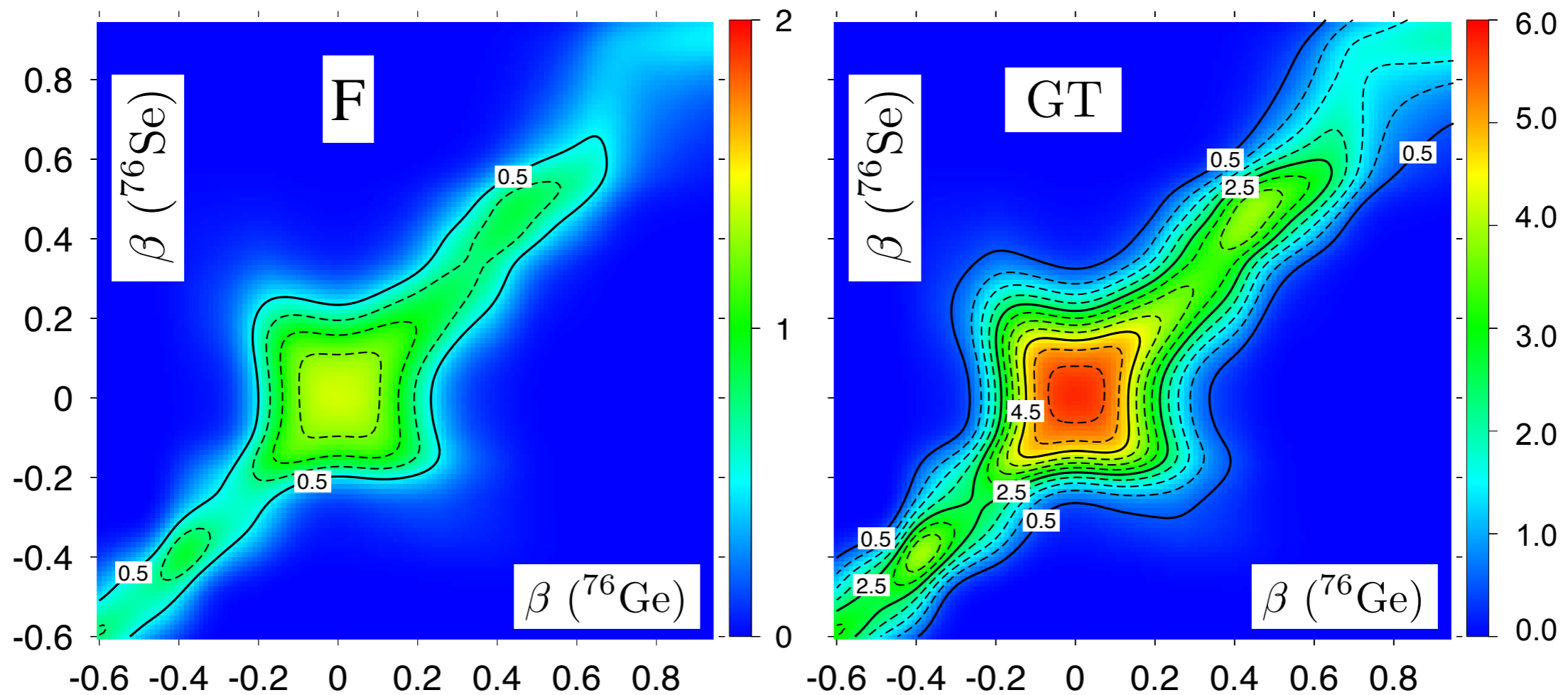


- GT strength greater than Fermi.
- Similar deformation between mother and granddaughter is favored by the transition operators
- Maxima are found close to sphericity although some other local maxima are found
- Final result depends on the distribution of probability of the corresponding initial and final collective states within this plot

NME: deformation and mixing

$$\frac{\langle 0; N_f Z_f; q_f | \hat{O}_\xi^{0\nu\beta\beta} | 0; N_i Z_i; q_i \rangle}{\sqrt{\langle 0; N_f Z_f; q_f | 0; N_f Z_f; q_f \rangle \langle 0; N_i Z_i; q_i | 0; N_i Z_i; q_i \rangle}}$$

A=76

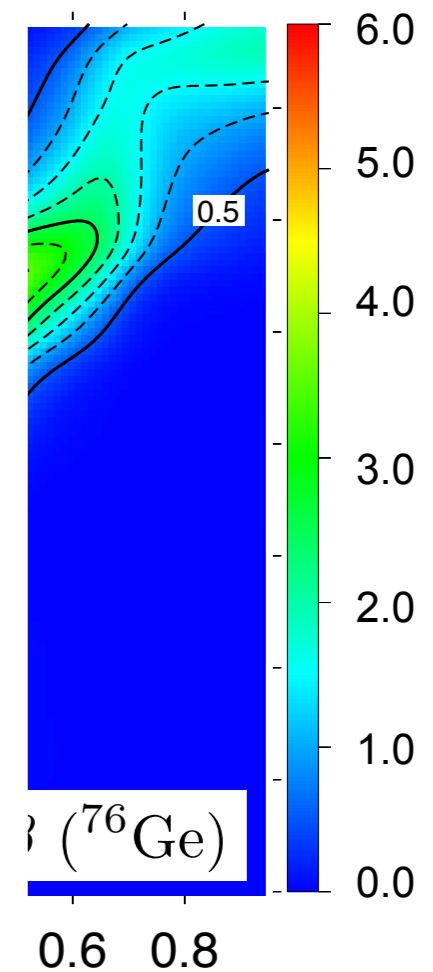
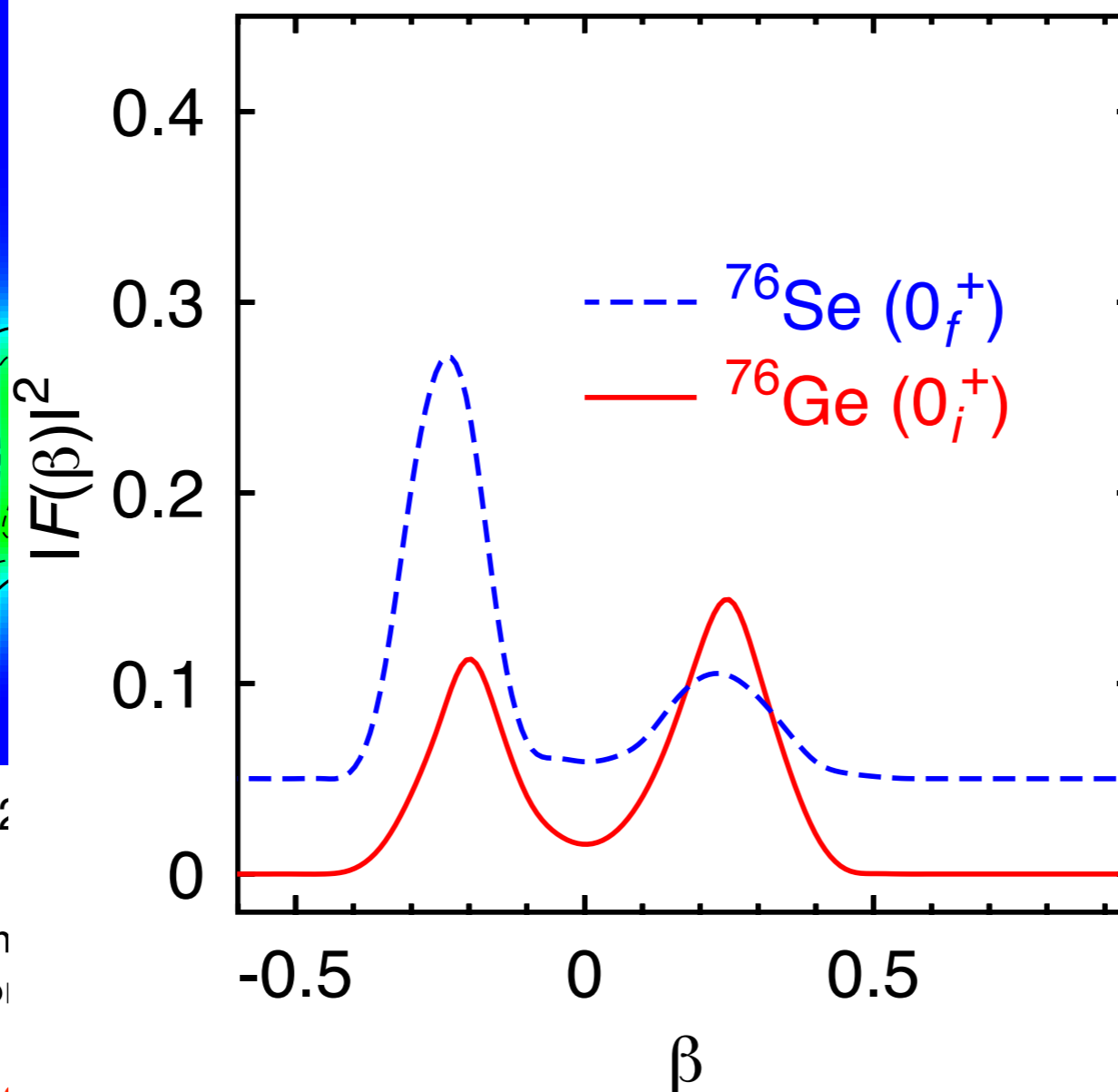
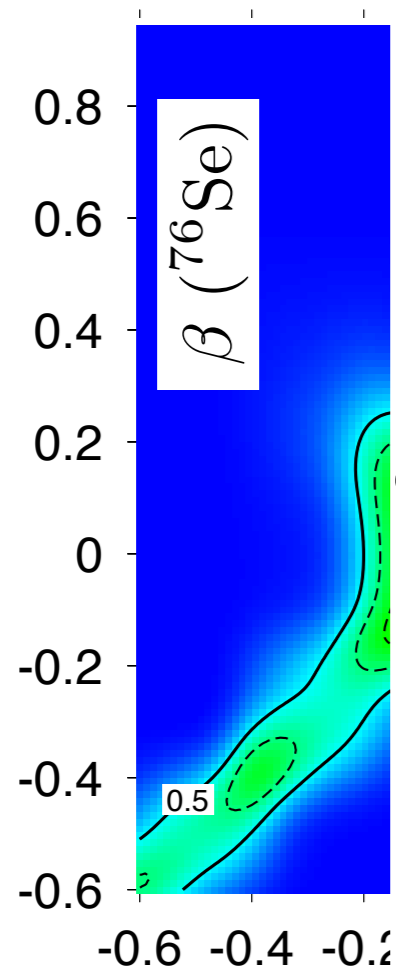


- GT strength greater than Fermi.
- Similar deformation between mother and granddaughter is favored by the transition operators
- Maxima are found close to sphericity although some other local maxima are found

NME: deformation and mixing

$$\frac{\langle 0; N_f Z_f; q_f | \hat{O}_\xi^{0\nu\beta\beta} | 0; N_i Z_i; q_i \rangle}{\sqrt{\langle 0; N_f Z_f; q_f | 0; N_f Z_f; q_f \rangle \langle 0; N_i Z_i; q_i | 0; N_i Z_i; q_i \rangle}}$$

A=76



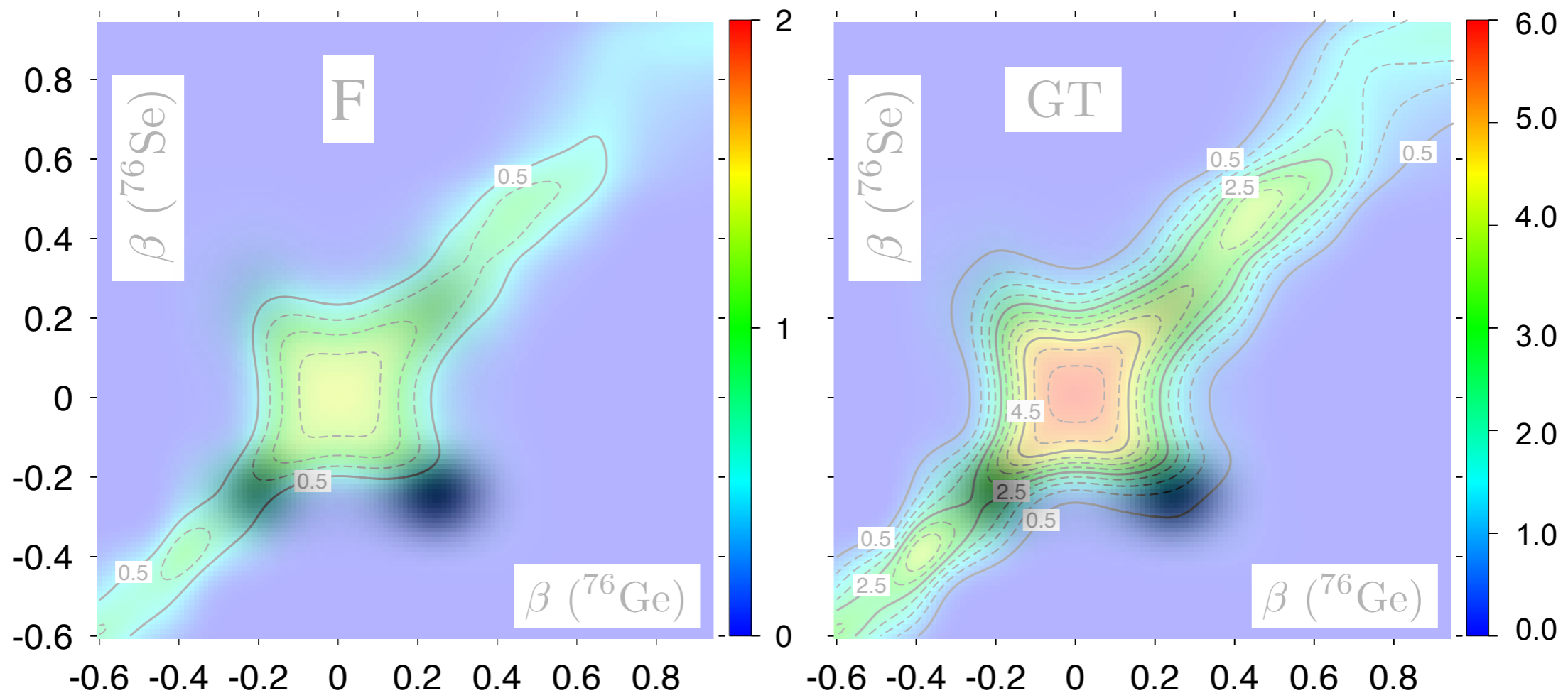
- GT strength
- Similar deformation
- Maxima are
- Final result of
- states within

ion operators
and
and final collective

NME: deformation and mixing

$$\frac{\langle 0; N_f Z_f; q_f | \hat{O}_\xi^{0\nu\beta\beta} | 0; N_i Z_i; q_i \rangle}{\sqrt{\langle 0; N_f Z_f; q_f | 0; N_f Z_f; q_f \rangle \langle 0; N_i Z_i; q_i | 0; N_i Z_i; q_i \rangle}}$$

A=76

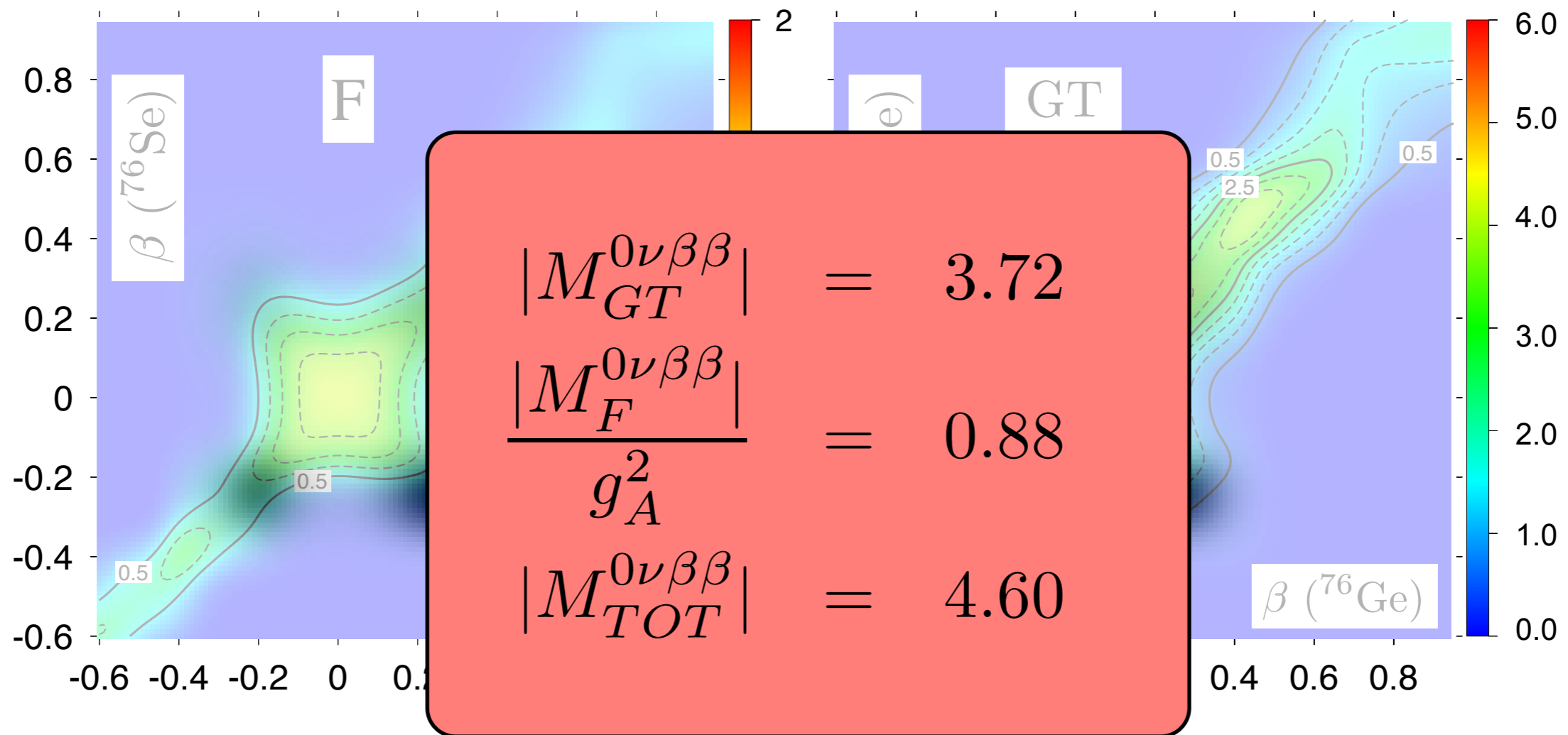


- GT strength greater than Fermi.
- Similar deformation between mother and granddaughter is favored by the transition operators
- Maxima are found close to sphericity although some other local maxima are found
- Final result depends on the distribution of probability of the corresponding initial and final collective states within this plot

NME: deformation and mixing

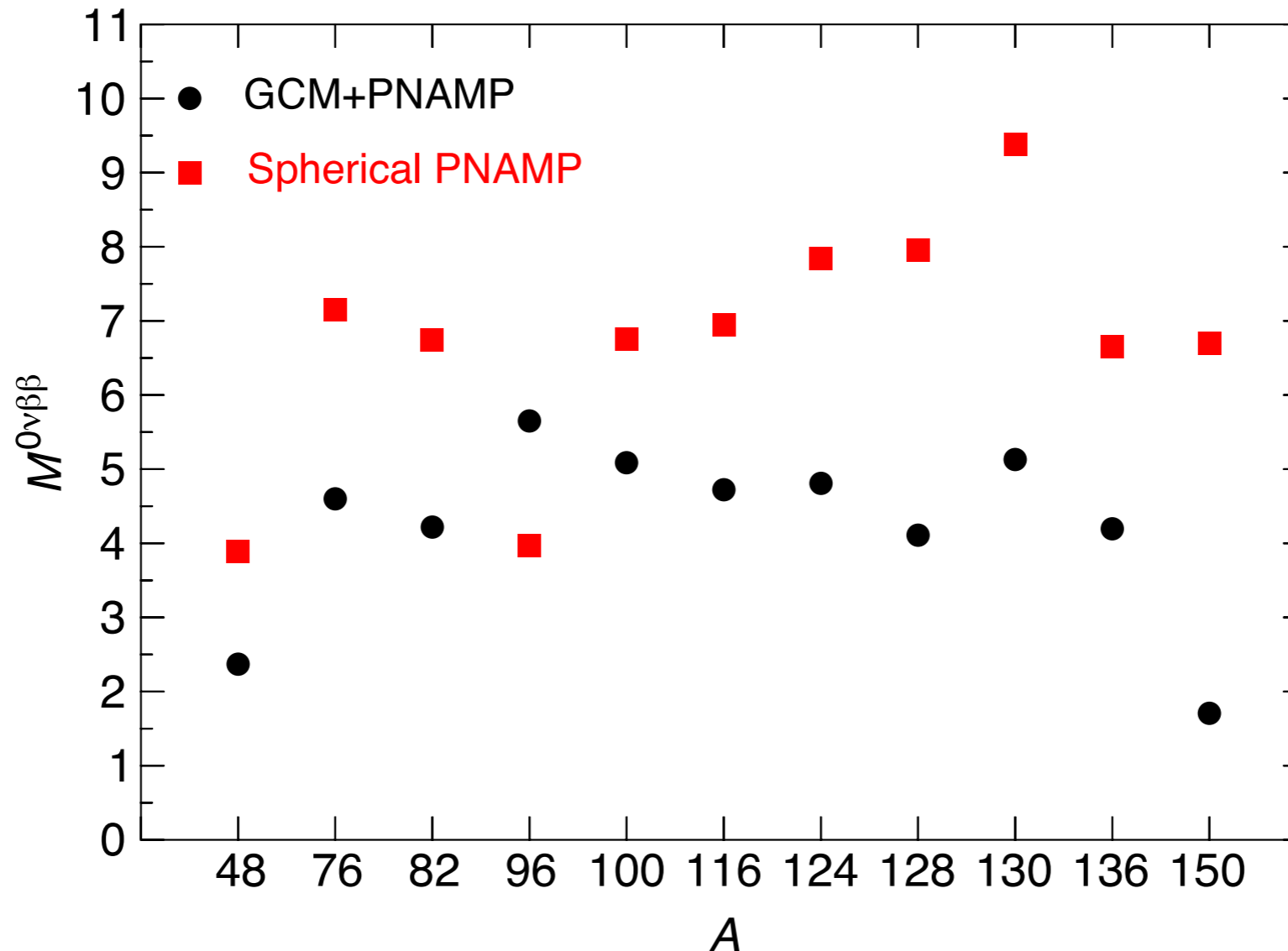
$$\frac{\langle 0; N_f Z_f; q_f | \hat{O}_\xi^{0\nu\beta\beta} | 0; N_i Z_i; q_i \rangle}{\sqrt{\langle 0; N_f Z_f; q_f | 0; N_f Z_f; q_f \rangle \langle 0; N_i Z_i; q_i | 0; N_i Z_i; q_i \rangle}}$$

A=76



- GT strength greater than Fermi.
- Similar deformation between mother and granddaughter is favored by the transition operators
- Maxima are found close to sphericity although some other local maxima are found
- Final result depends on the distribution of probability of the corresponding initial and final collective states within this plot

NME: deformation and mixing



Noticeable difference in the NME if only intrinsic spherical configurations are considered without configuration mixing.

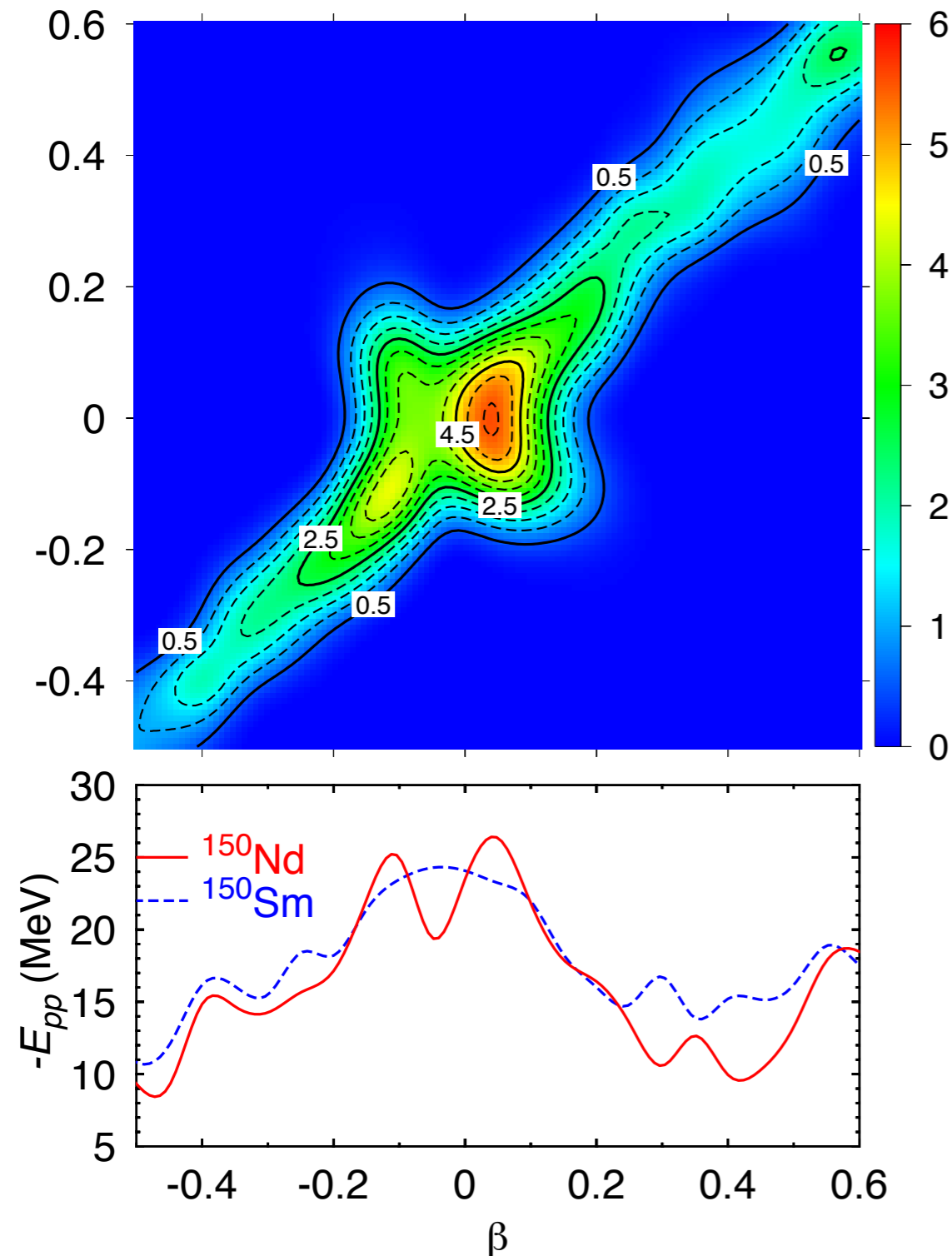
NME: Pairing

I. Introduction

2. Method: GCM+PNAMP

3. Results: GCM+PNAMP

4. Summary and Conclusions



- The structure is related to the pairing energy (particle-particle) of the nuclei involved in the transition
- Maxima of the strength correspond to maxima in pairing energy
- In agreement with seniority arguments (increasing seniority decreases NME)
- Pairing energy and NME involve similar Wick theorem's contractions in this formalism

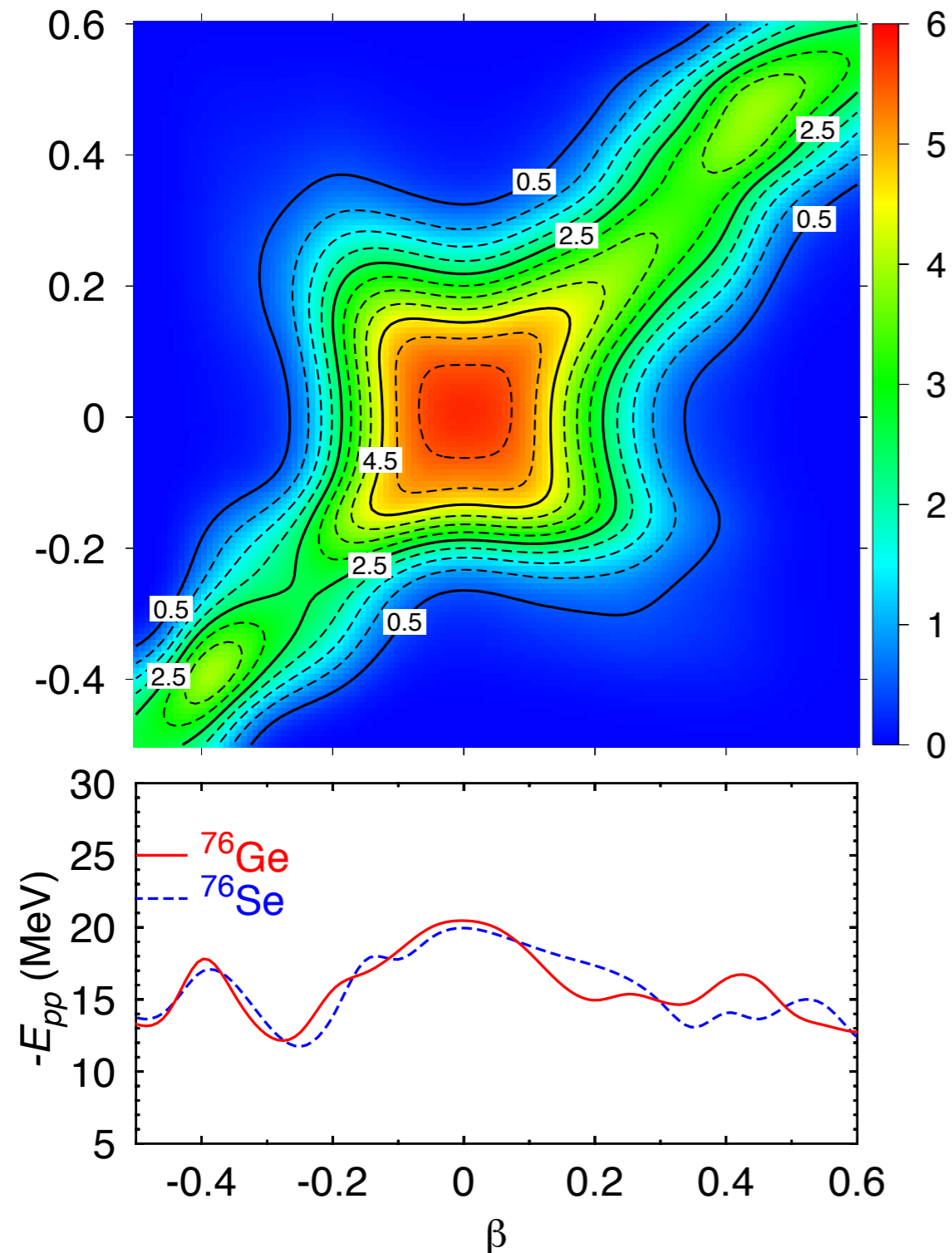
NME: Pairing

I. Introduction

2. Method: GCM+PNAMP

3. Results: GCM+PNAMP

4. Summary and Conclusions



- The structure is related to the pairing energy (particle-particle) of the nuclei involved in the transition
- Maxima of the strength correspond to maxima in pairing energy
- In agreement with seniority arguments (increasing seniority decreases NME)
- Pairing energy and NME involve similar Wick theorem's contractions in this formalism

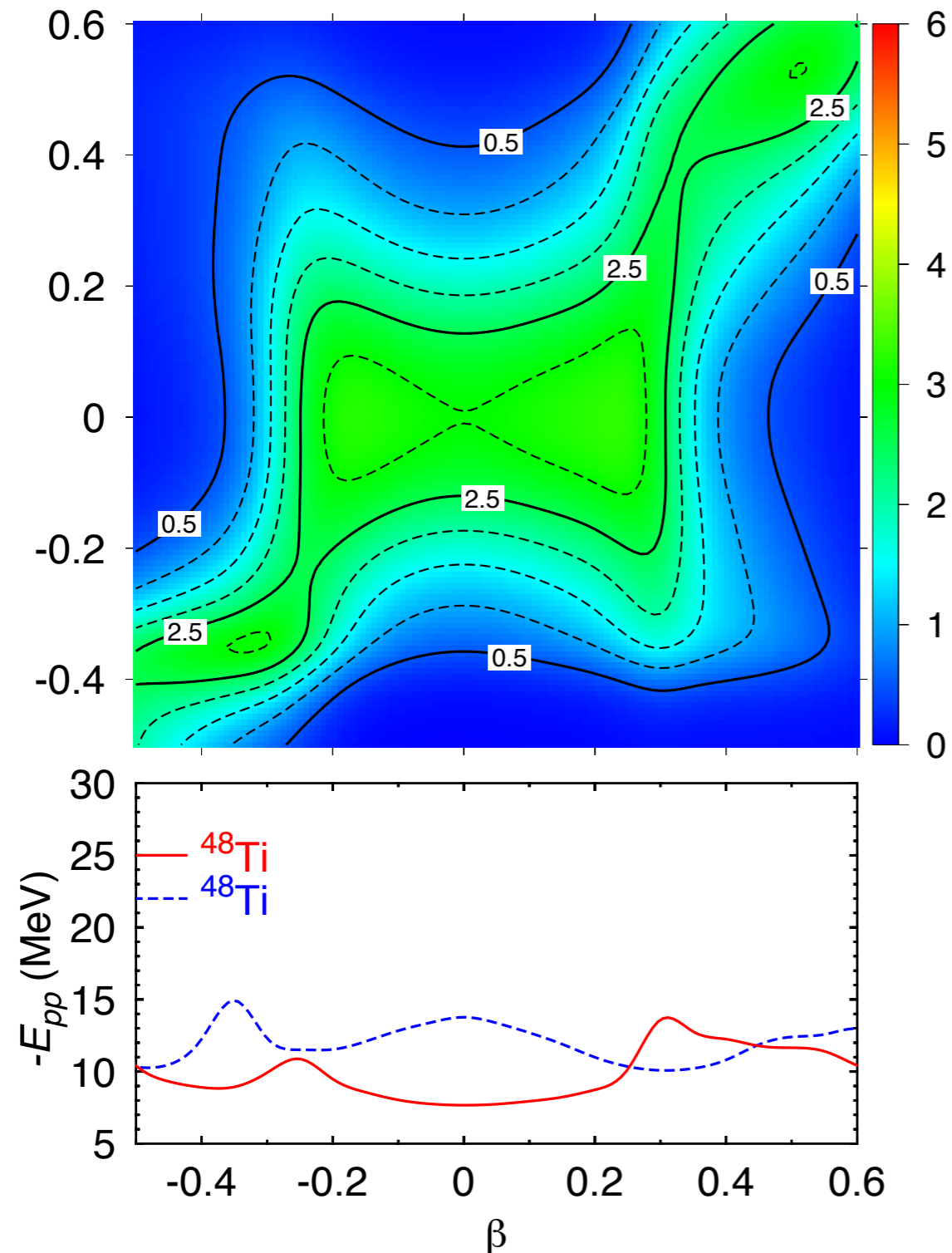
NME: Pairing

I. Introduction

2. Method: GCM+PNAMP

3. Results: GCM+PNAMP

4. Summary and Conclusions



- The structure is related to the pairing energy (particle-particle) of the nuclei involved in the transition
- Maxima of the strength correspond to maxima in pairing energy
- In agreement with seniority arguments (increasing seniority decreases NME)
- Pairing energy and NME involve similar Wick theorem's contractions in this formalism

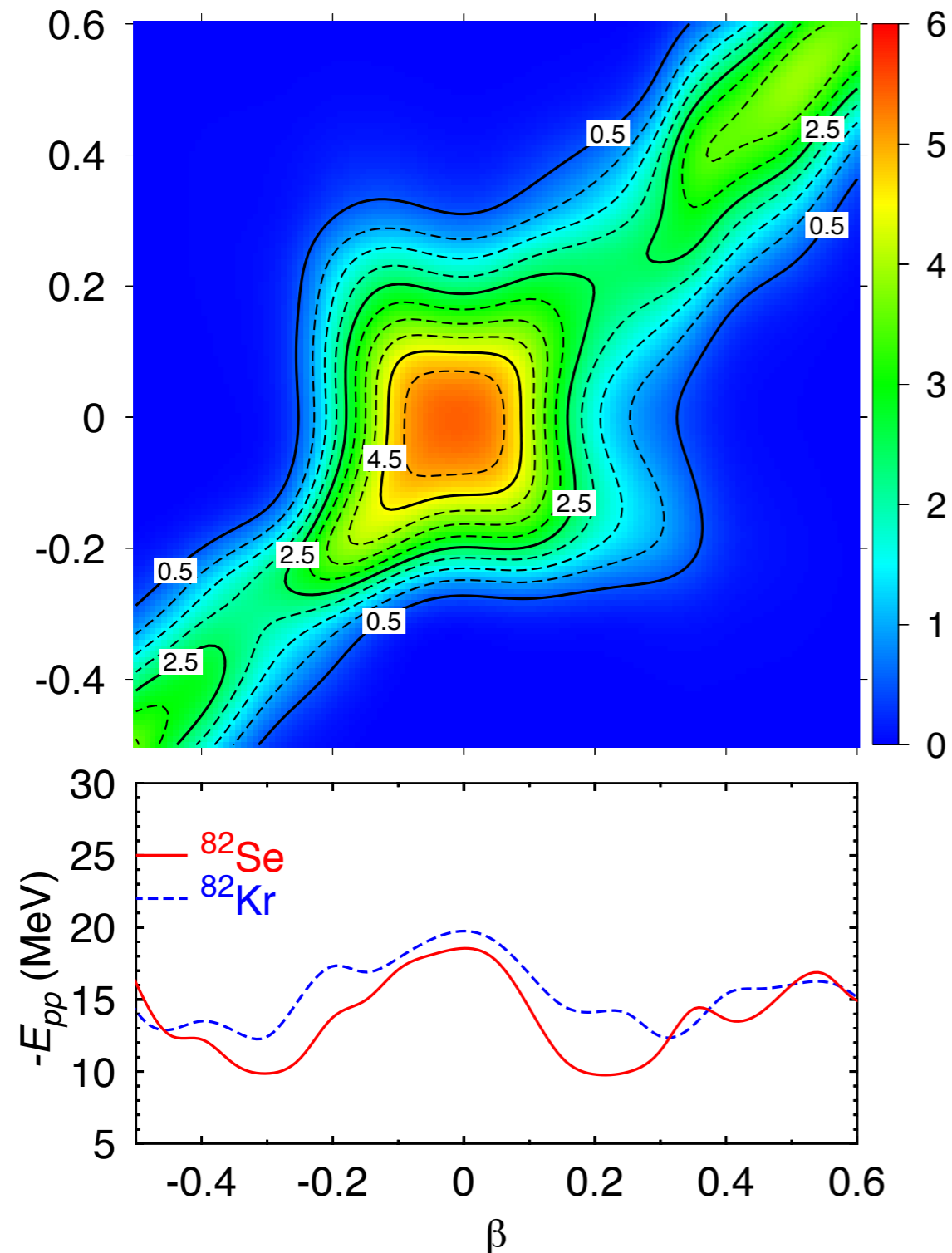
NME: Pairing

I. Introduction

2. Method: GCM+PNAMP

3. Results: GCM+PNAMP

4. Summary and Conclusions



- The structure is related to the pairing energy (particle-particle) of the nuclei involved in the transition
- Maxima of the strength correspond to maxima in pairing energy
- In agreement with seniority arguments (increasing seniority decreases NME)
- Pairing energy and NME involve similar Wick theorem's contractions in this formalism

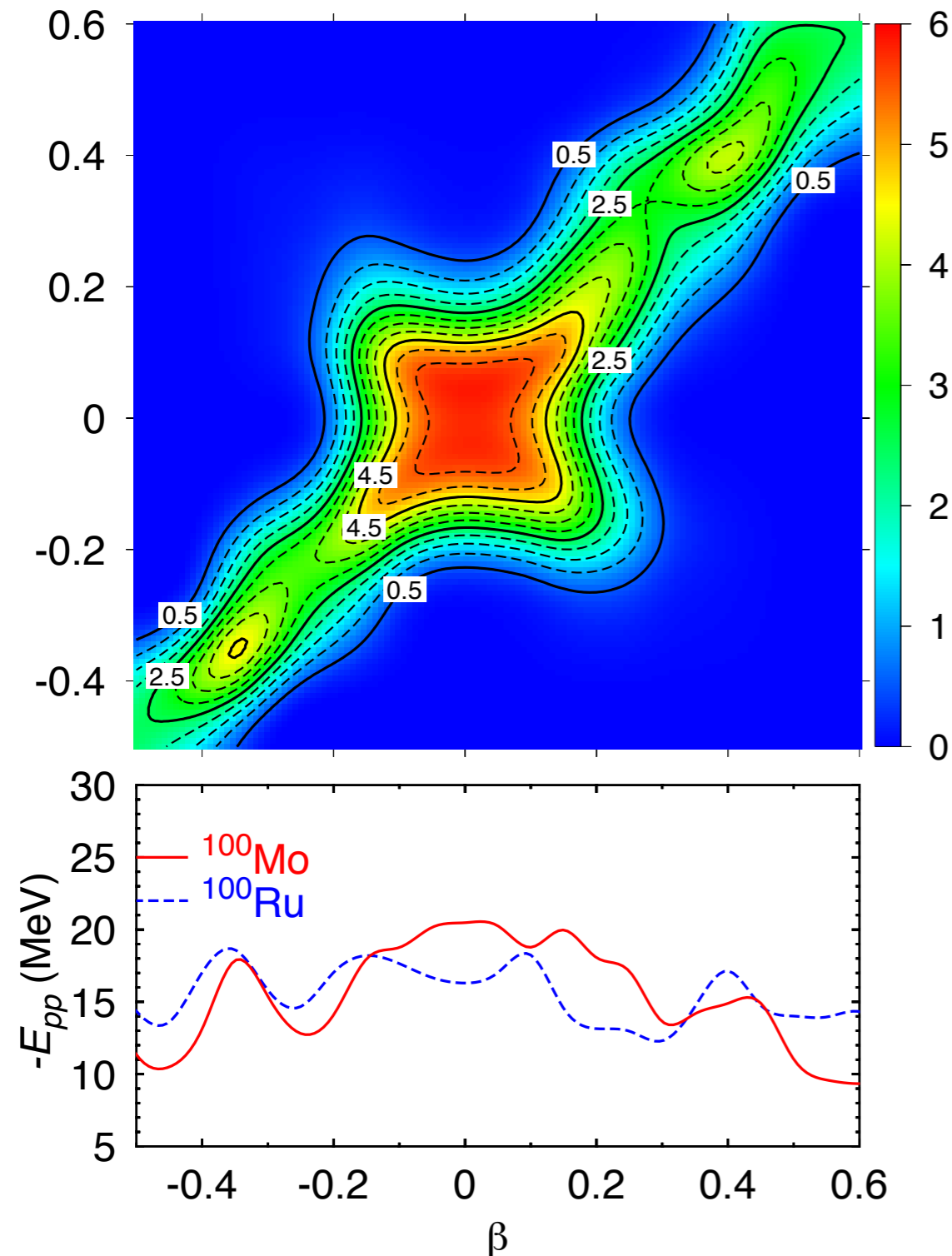
NME: Pairing

I. Introduction

2. Method: GCM+PNAMP

3. Results: GCM+PNAMP

4. Summary and Conclusions



- The structure is related to the pairing energy (particle-particle) of the nuclei involved in the transition
- Maxima of the strength correspond to maxima in pairing energy
- In agreement with seniority arguments (increasing seniority decreases NME)
- Pairing energy and NME involve similar Wick theorem's contractions in this formalism

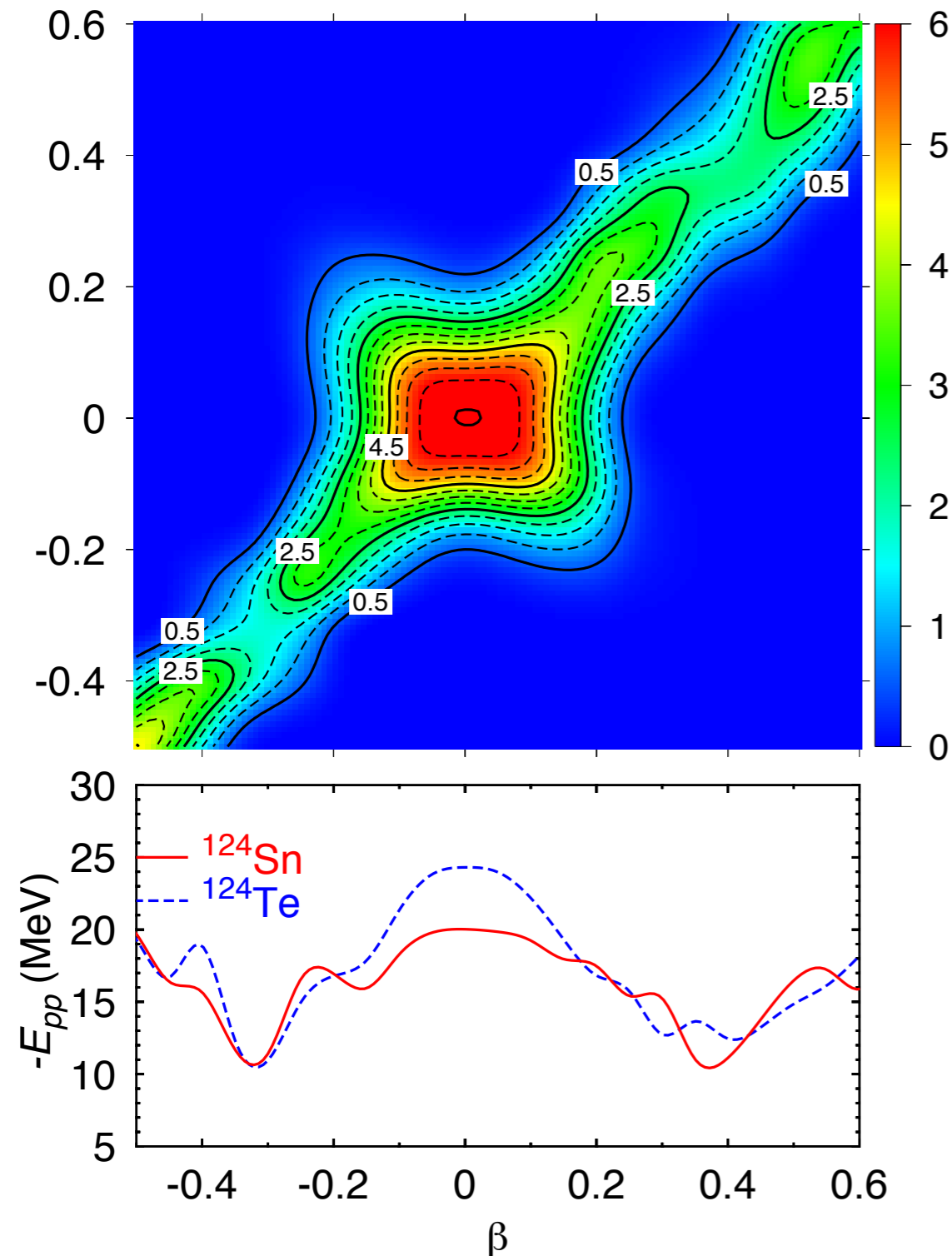
NME: Pairing

I. Introduction

2. Method: GCM+PNAMP

3. Results: GCM+PNAMP

4. Summary and Conclusions



- The structure is related to the pairing energy (particle-particle) of the nuclei involved in the transition
- Maxima of the strength correspond to maxima in pairing energy
- In agreement with seniority arguments (increasing seniority decreases NME)
- Pairing energy and NME involve similar Wick theorem's contractions in this formalism

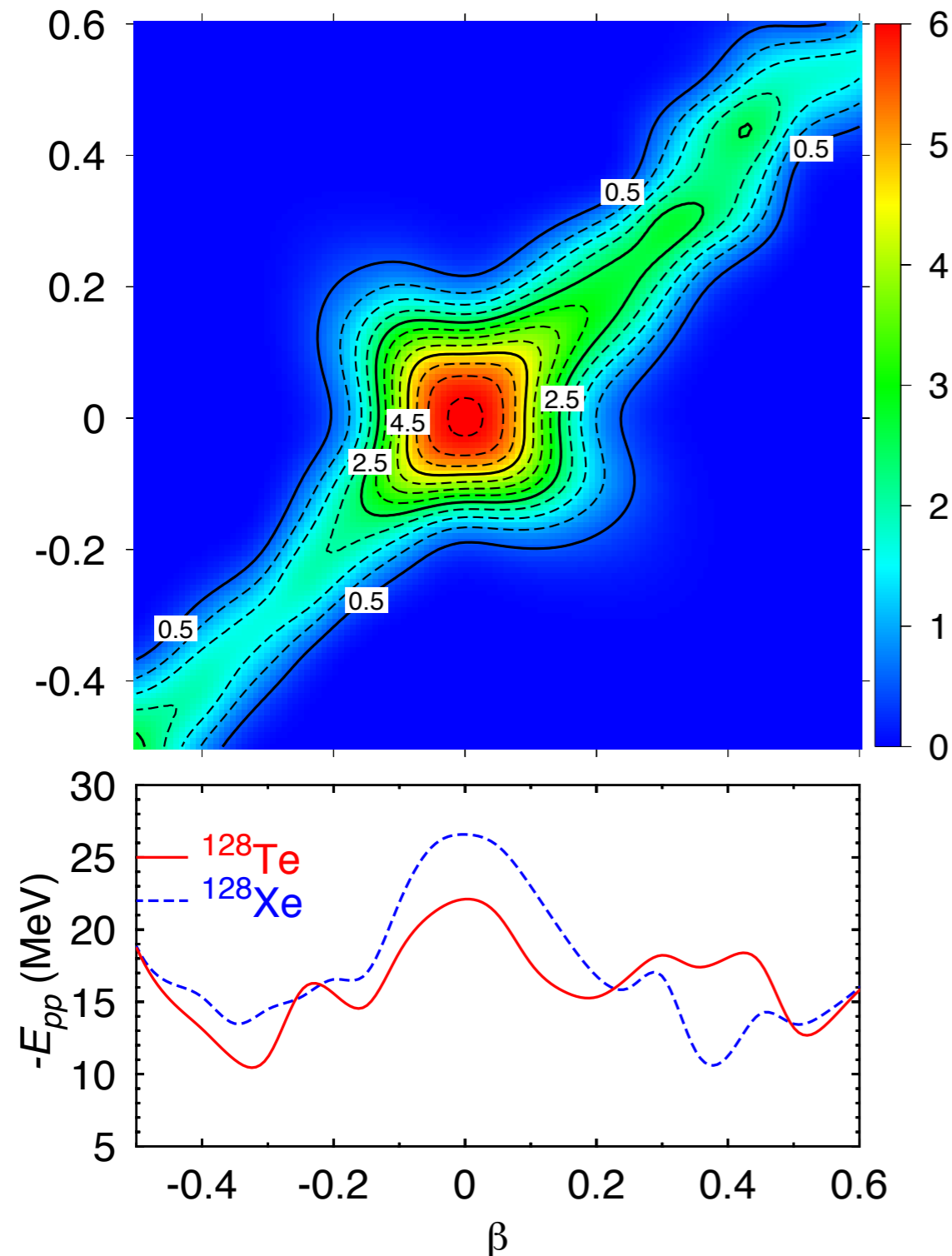
NME: Pairing

I. Introduction

2. Method: GCM+PNAMP

3. Results: GCM+PNAMP

4. Summary and Conclusions



- The structure is related to the pairing energy (particle-particle) of the nuclei involved in the transition
- Maxima of the strength correspond to maxima in pairing energy
- In agreement with seniority arguments (increasing seniority decreases NME)
- Pairing energy and NME involve similar Wick theorem's contractions in this formalism

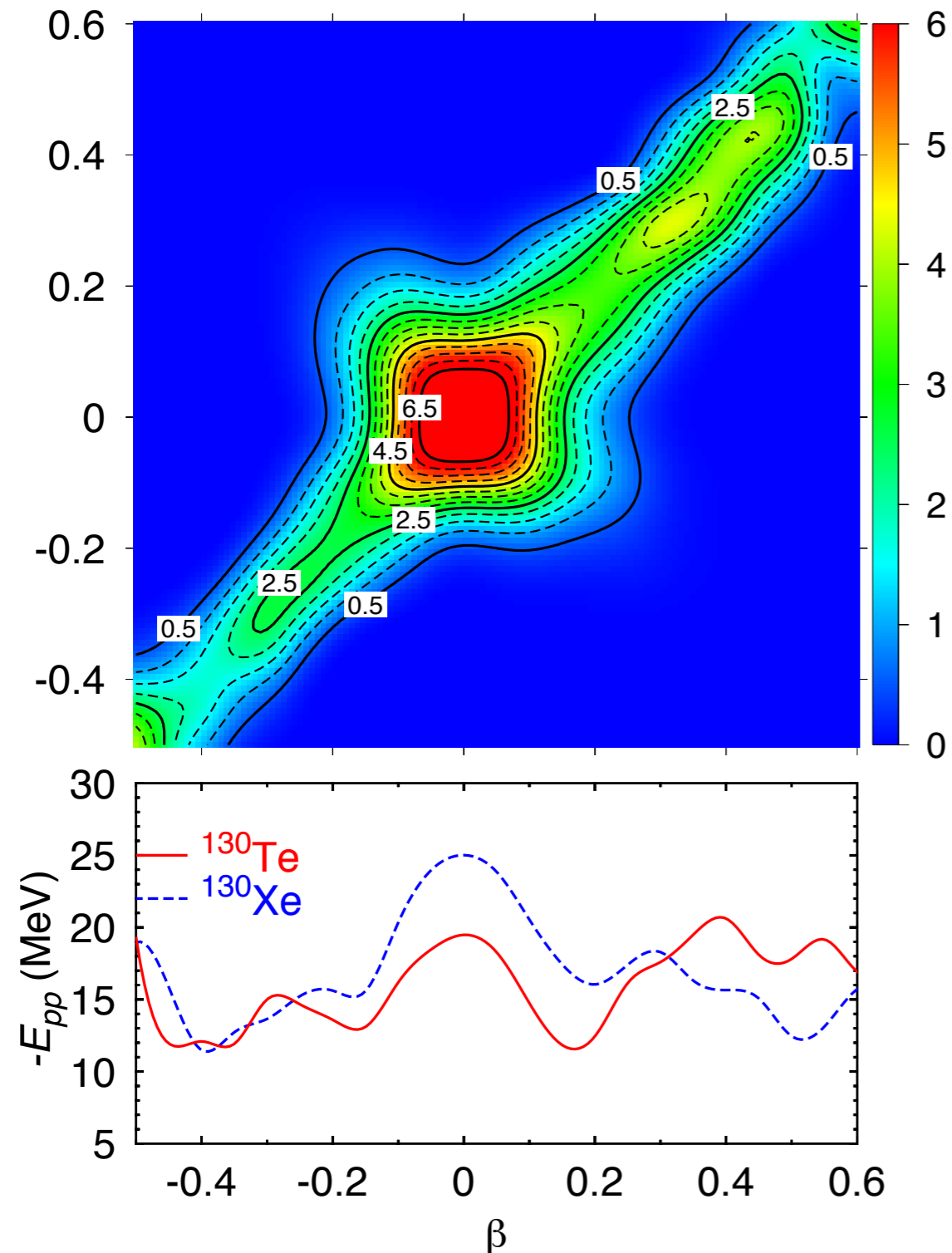
NME: Pairing

I. Introduction

2. Method: GCM+PNAMP

3. Results: GCM+PNAMP

4. Summary and Conclusions



- The structure is related to the pairing energy (particle-particle) of the nuclei involved in the transition
- Maxima of the strength correspond to maxima in pairing energy
- In agreement with seniority arguments (increasing seniority decreases NME)
- Pairing energy and NME involve similar Wick theorem's contractions in this formalism

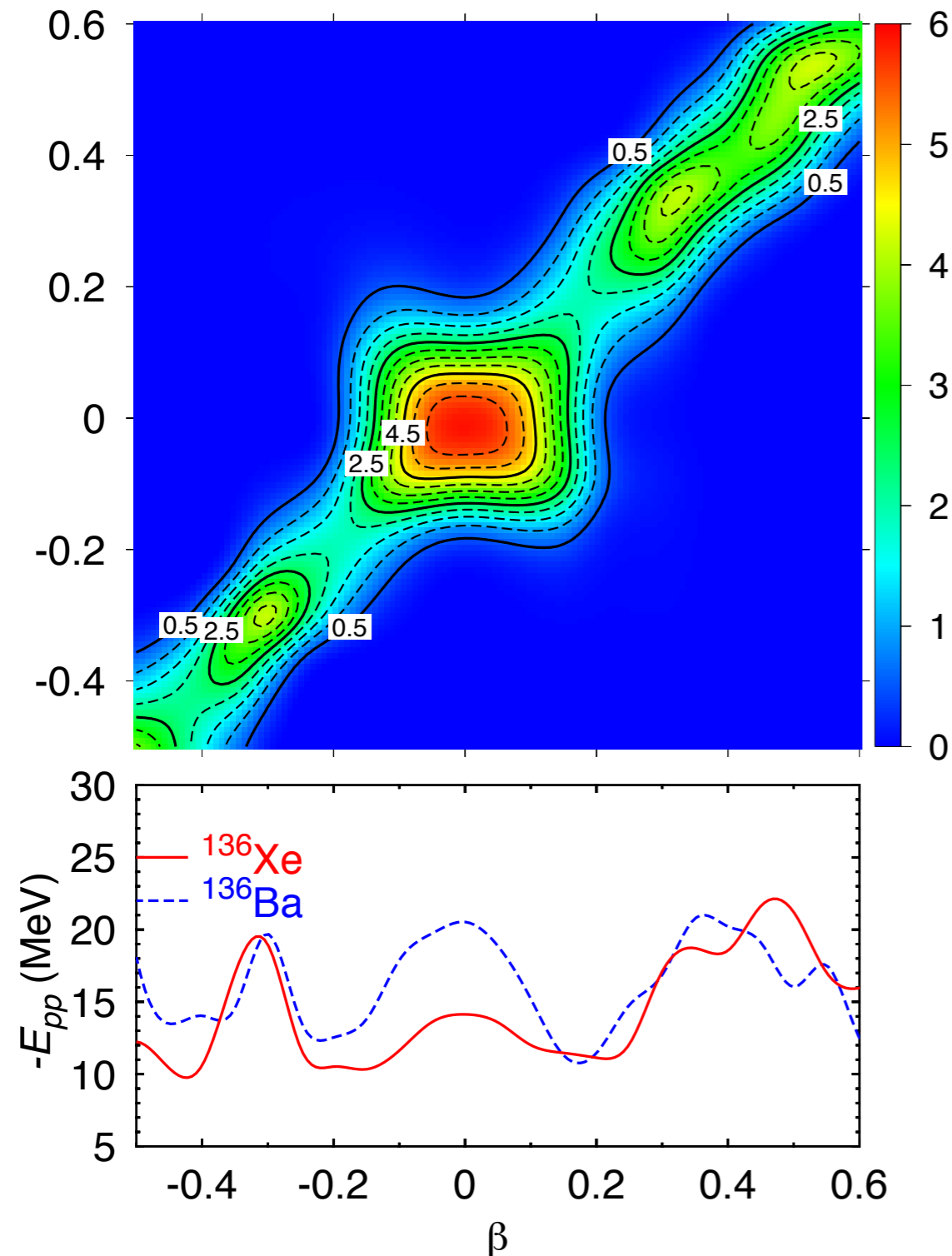
NME: Pairing

I. Introduction

2. Method: GCM+PNAMP

3. Results: GCM+PNAMP

4. Summary and Conclusions



- The structure is related to the pairing energy (particle-particle) of the nuclei involved in the transition
- Maxima of the strength correspond to maxima in pairing energy
- In agreement with seniority arguments (increasing seniority decreases NME)
- Pairing energy and NME involve similar Wick theorem's contractions in this formalism

NME: Pairing

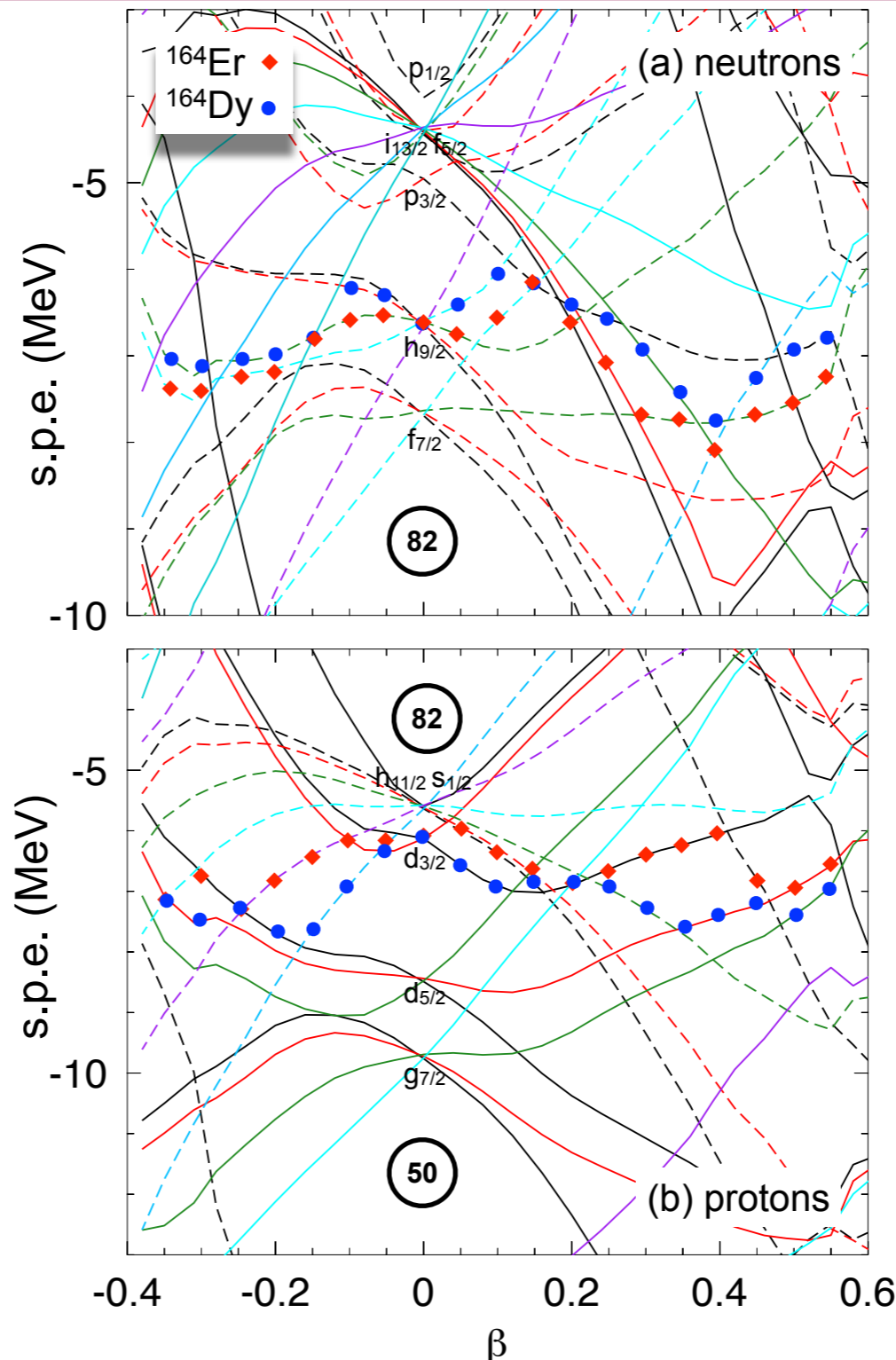
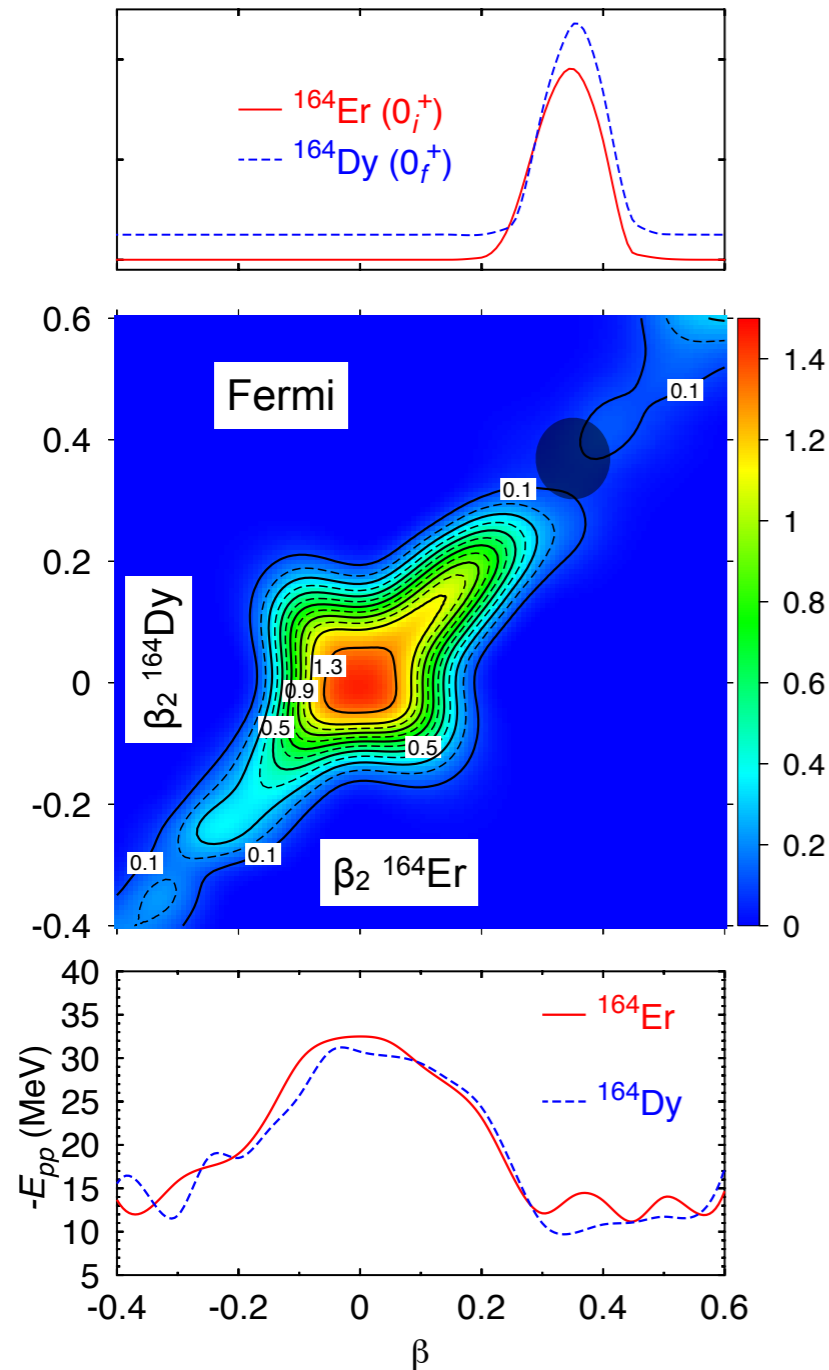
I. Introduction

2. Method: GCM+PNAMP

3. Results: GCM+PNAMP

4. Summary and Conclusions

T.R.R., G. Martínez-Pinedo, PRC 2012



- The minima (maxima) of the NME as a function of deformation are related to areas with low (high) level density around the Fermi level of the initial and final states.

NME: Pairing

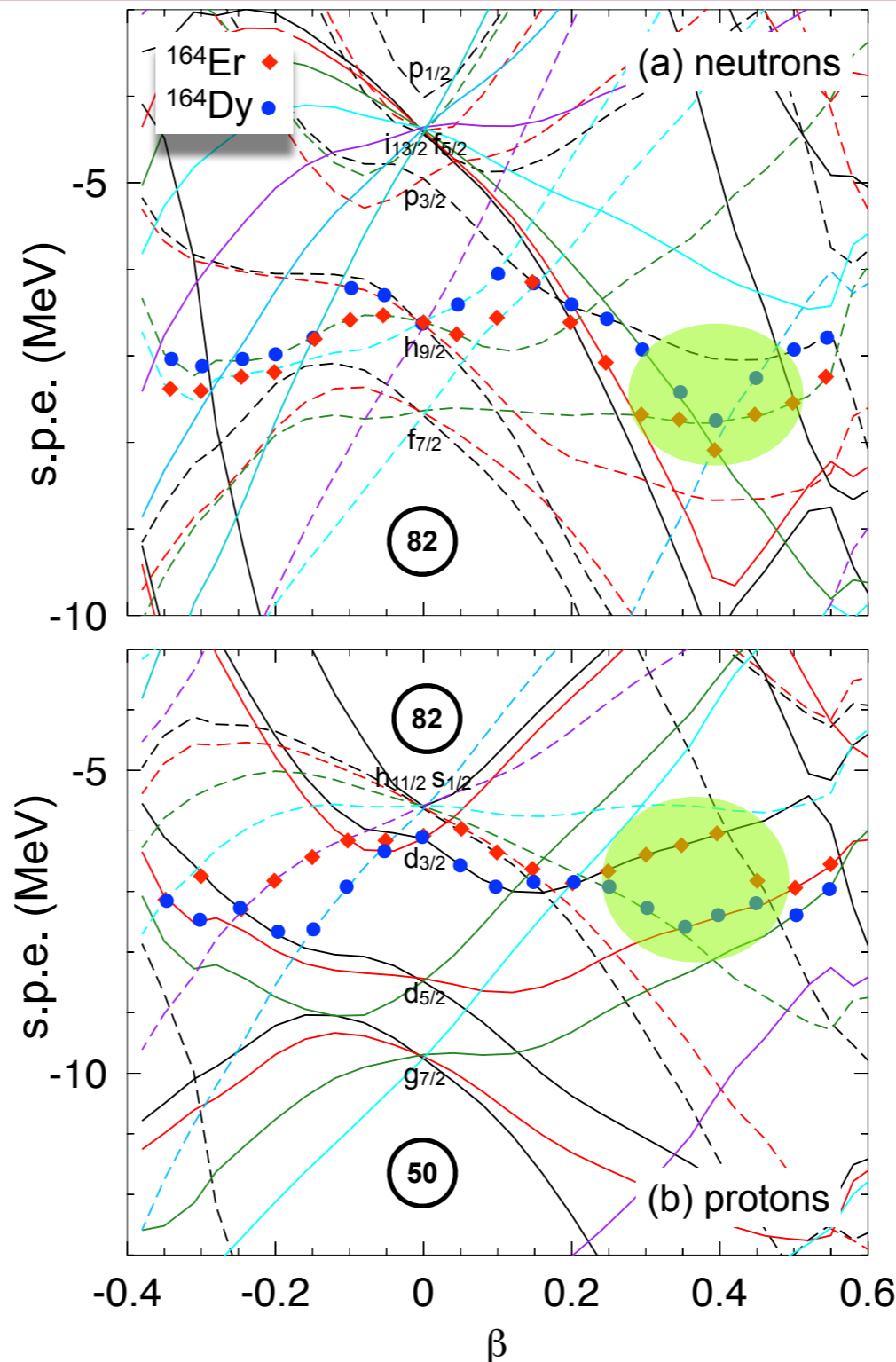
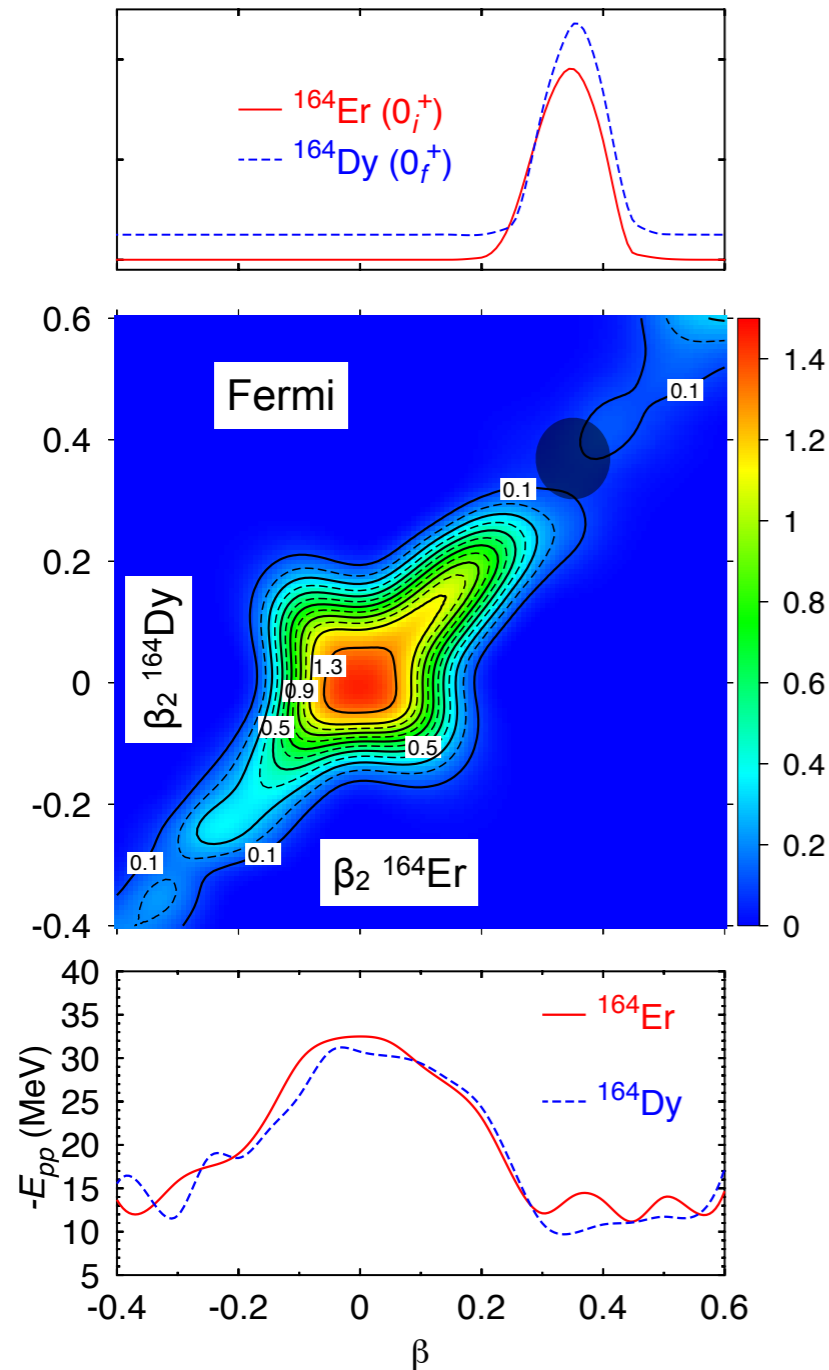
I. Introduction

2. Method: GCM+PNAMP

3. Results: GCM+PNAMP

4. Summary and Conclusions

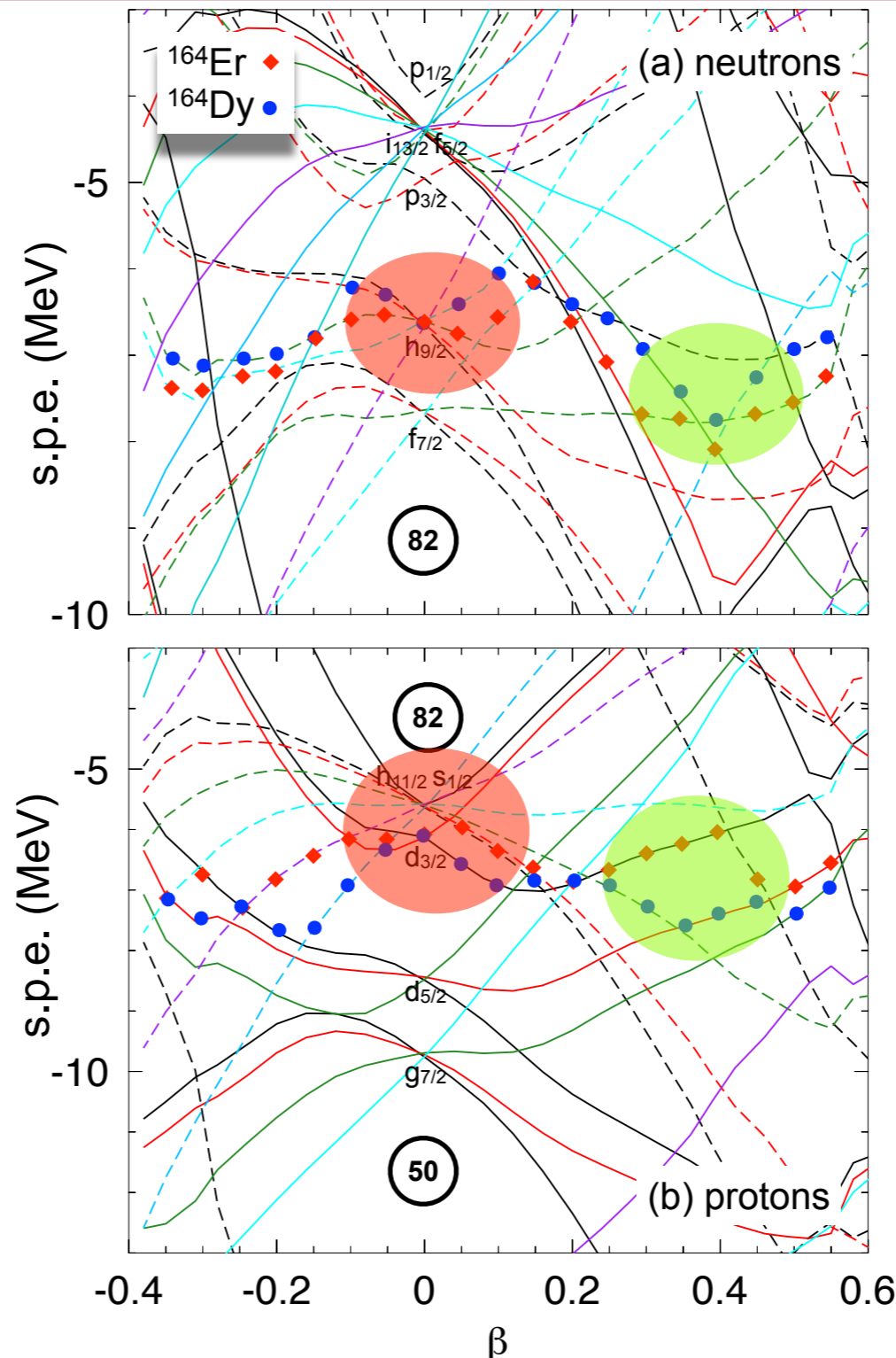
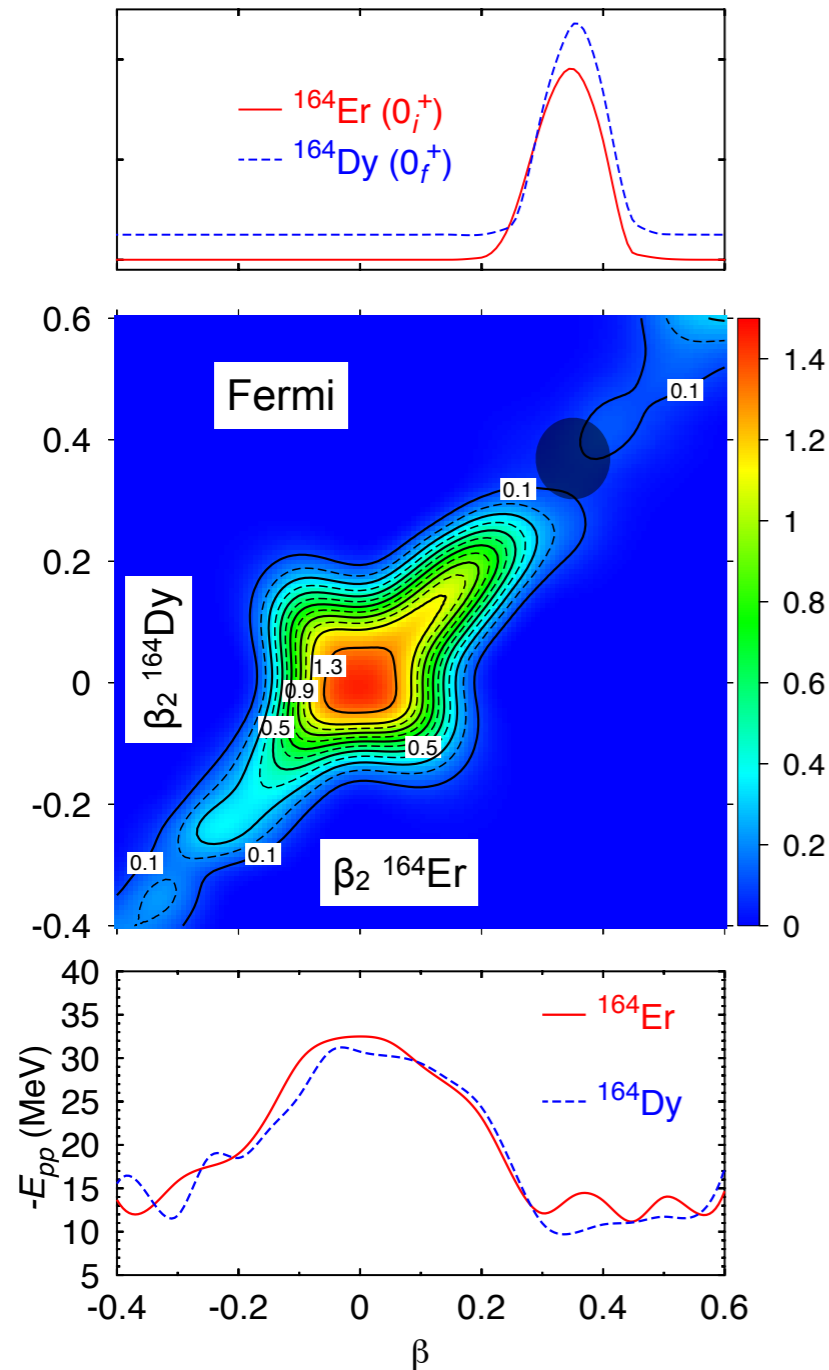
T.R.R., G. Martínez-Pinedo, PRC 2012



- The minima (maxima) of the NME as a function of deformation are related to areas with low (high) level density around the Fermi level of the initial and final states.

NME: Pairing

T.R.R., G. Martínez-Pinedo, PRC 2012



- The minima (maxima) of the NME as a function of deformation are related to areas with low (high) level density around the Fermi level of the initial and final states.

NME: Summary of the results

Gogny DIS parametrization

A	48	76	82	96	100	116	124	128	130	136	150	152	164	180
$M^{0\nu}$	2.37	4.60	4.22	5.65	5.08	4.72	4.81	4.11	5.13	4.20	1.71	1.07	0.64	0.58
$T_{1/2}$ (y)	28.5×10^{23}	76.9×10^{23}	20.8×10^{23}	5.48×10^{23}	8.64×10^{23}	9.24×10^{23}	16.2×10^{23}	343.1×10^{23}	8.84×10^{23}	12.7×10^{23}	16.5×10^{23}	4.2×10^{31}	1.3×10^{36}	1.6×10^{34}

Gogny DIM parametrization

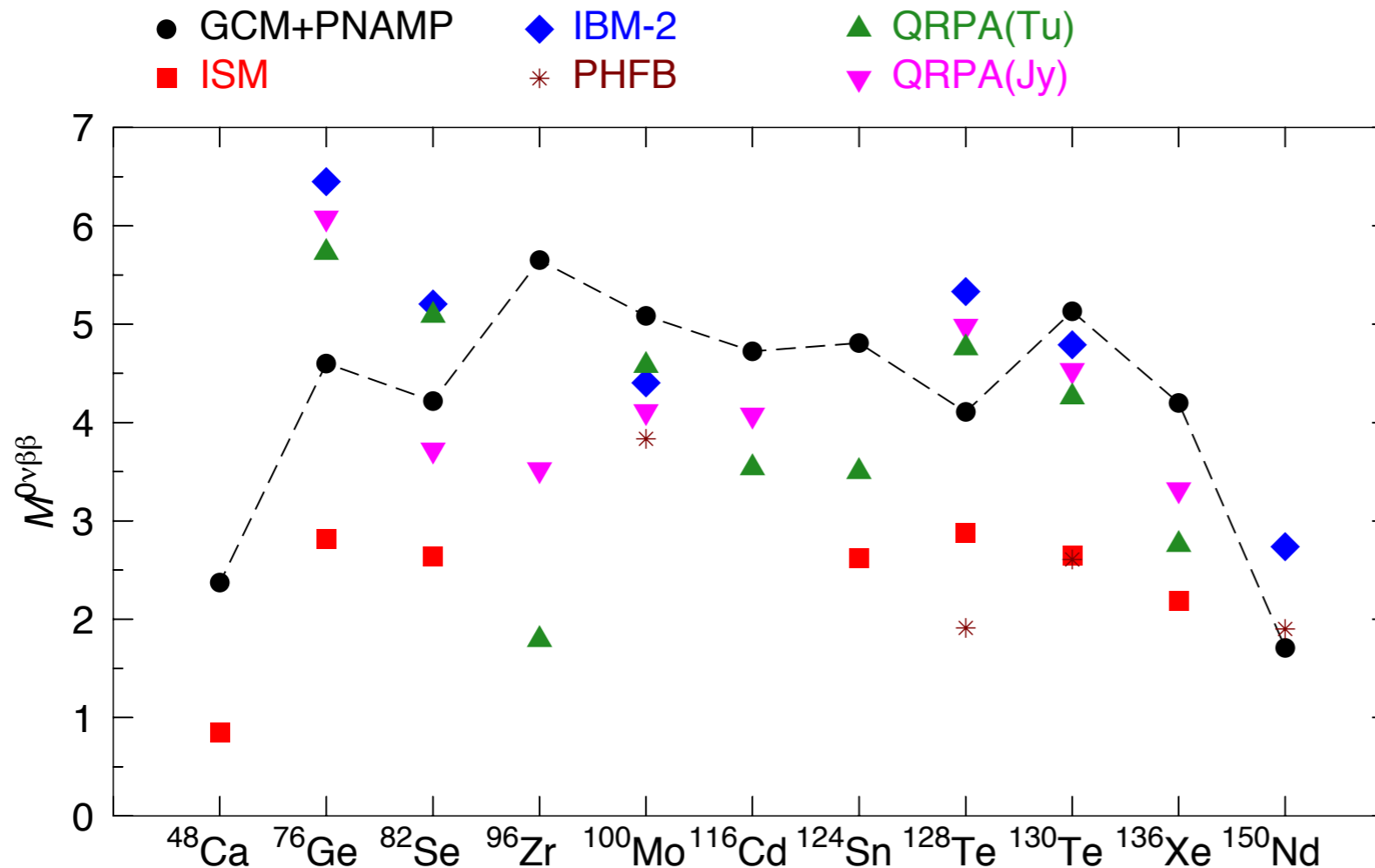
A	48	76	82	96	100	116	124	128	130	136	150	152	164	180
$M^{0\nu}$	2.43	4.64	4.28	5.70	5.19	4.83	4.71	3.98	5.07	4.29	1.36	0.89	0.50	0.38
$T_{1/2}$ (y)	27.1×10^{23}	75.6×10^{23}	20.2×10^{23}	5.38×10^{23}	8.28×10^{23}	8.82×10^{23}	16.9×10^{23}	365.8×10^{23}	9.05×10^{23}	12.2×10^{23}	26.1×10^{23}	6.2×10^{31}	2.1×10^{36}	3.8×10^{34}

double beta decay

double electron capture

NME: Summary of the results

T.R.R., Martínez-Pinedo, PRL 2010



QRPA (Jy): J.M. Kortelainen, J. Suhonen, PRC 75, 051303(R) (2007) and PRC 76, 024315 (2007)

QRPA(Tu): F. Simkovic et al., PRC 77, 045503 (2008)

ISM: J. Menendez et al., PRL 100, 52503 (2008)

IBM-2: J. Barea, F. Iachello, PRC 77, 045503 (2008)

PHFB: K. Chaturvedi et al. PRC 78, 054302 (2008)

- Higher values than the ones predicted by ISM calculations (larger valence space, lower seniority components).
- For $A=76, 82, 128, 150$ we predict smaller values than the ones given by QRPA and/or IBM while for $A=96, 100, 116, 124, 130, 136$ larger values are obtained.
- Consistent results with the rest of the models. Notice that we are using the same interaction for all the nuclei.
- Further studies are needed to understand what is missing in the different models.

NME: Summary of the results

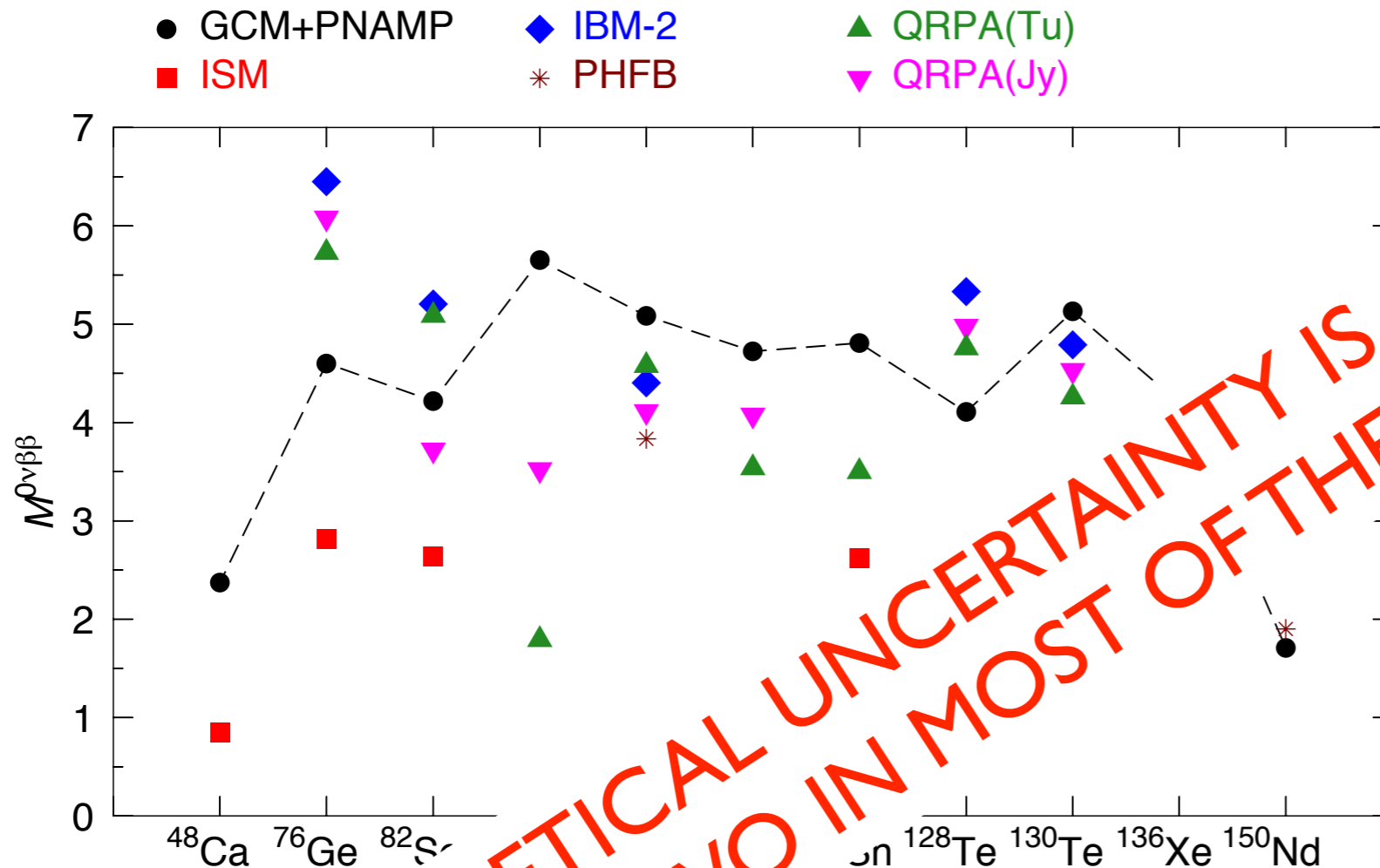
I. Introduction

2. Method: GCM+PNAMP

3. Results: GCM+PNAMP

4. Summary and Conclusions

T.R.R., Martínez-Pinedo, PRL 2010



QRPA (Jy): M. Kortelainen, J. Suhonen, PRC 76, 051303(R) (2008)

QRPA (Tu): M. Kortelainen, J. Suhonen, PRC 76, 051303(R) (2008)

IBM-2: J. Barea, F. Iachello, PRC 77, 045503 (2008)

ISM: J. Menendez et al., PRL 100, 52503 (2008)

PHFB: K. Chaturvedi et al., PRC 78, 054302 (2008)

- Higher values are obtained by ISM calculations (larger valence space, lower seniority component)
- For $A=76$ and 82 we predict smaller values than the ones given by QRPA and/or IBM while for $A=96, 100, 116, 130, 136$ larger values are obtained.
- Consistent results with the rest of the models. Notice that we are using the same interaction for all the nuclei.
- Further studies are needed to understand what is missing in the different models.

Summary and conclusions

- Energy density functional methods allow the inclusion of deformation of the initial and final states in the calculation of NME for neutrinoless double beta decay and double electron capture.
- Equal deformation of initial and final states is favored by the transition operator. Spherical configurations are more favored than deformed ones.
- NME values are strongly correlated to the pairing energies of initial and final states.
- NMEs are much larger for the double beta decay candidates than for double electron capture ones (deformation).

Outlook

- Calculations in the pf-shell.
- Other degrees of freedom should be also explored (pairing vibrations, octupole deformations, triaxiality, explicit quasiparticle excitations...)
- Isospin symmetry breaking and restoration.
- Occupation numbers.

Acknowledgments

G. Martínez-Pinedo (TU-Darmstadt)

K. Blaum (Universität Heidelberg)

T. Duguet (CEA-Saclay)

J. L. Egido (UAM-Madrid)

K. Langanke (GSI-Darmstadt)

N. López-Vaquero (UAM-Madrid)

J. Menéndez (TU Darmstadt)

F. Nowacki (Strasbourg)

A. Poves (UAM-Madrid)

C. Smorra (Universität Heidelberg)